POWER ELECTRONICS EUROPE

ISSUE 8 – December 2013 www.power-mag.com

POWER SUPPLY DESIGN

Achieving a Stable Power Supply with Fast Transient Response Through Digital Control

THE EUROPEAN JOURNAL FOR POWER ELECTRONICS AND TECHNOLOGY

Also inside this issue

Editor Achim Scharf
Tel: +49 (0)892865 9794
Fax: +49 (0)892800 132
Email: achimscharf@aol.com

Production Editor Chris Davis
Tel: +44 (0)1732 370340

Financial Manager Clare Jackson
Tel: +44 (0)1732 370340
Fax: +44 (0)1732 360034

Reader/Circulation Enquiries
Capsule Publishing Services Ltd
Tel: 0333 577 0801 Fax: 0845 604 2327
Email: circulation@capsule-group.com

INTERNATIONAL SALES OFFICES
Mainland Europe:
Victoria Hufmann, Norbert Hufmann
Tel: +49 911 9397 643 Fax: +49 911 9397 6459
Email: pee@hufmann.info

Armin Wezel
phone: +49 (0)30 52689192
mobile: +49 (0)172 767 8499
Email: armin@eurokom-media.d

Eastern US
Karen C Smith-Kernc
email: KarenKCS@aol.com
Western US and Canada
Alan A Kernc
Tel: +1 717 397 7100
Fax: +1 717 397 7800
email: AlanKCS@aol.com

Italy
Ferruccio Silvera
Tel: +39 022 846 716 Email: ferruccio@silvera.it

Japan:
Yoshinori Ikeda,
Pacific Business Inc
Tel: 81-(0)3-3661-6138
Fax: 81-(0)3-3661-6139
Email: pbi2010@gol.com

Taiwan
Prisco Ind. Service Corp.
Tel: 886 2 2322 5266 Fax: 886 2 2322 2205

Publisher & UK Sales Ian Atkinson
Tel: +44 (0)1732 370340
Fax: +44 (0)1732 360034
Email: ian@dfamedia.co.uk
www.power-mag.com

Circulation and subscription: **Power Electronics Europe** is available for the following subscription charges. **Power Electronics Europe**: annual charge UK/NI £60, overseas $130, EUR 120; single copies UK/NI £10, overseas US$32, EUR 25.
Contact: DFA Media, 192 The High Street, Tonbridge, Kent TN9 1BE Great Britain.
Tel: +44 (0)1732 370340.
Fax: +44 (0)1732 360034. Refunds on cancelled subscriptions will only be provided at the Publisher's discretion, unless specifically guaranteed within the terms of subscription offer.

Editorial information should be sent to The Editor, **Power Electronics Europe**, PO Box 340131, 80098 Munich, Germany.

Printed by: Garnett Dickinson.

ISSN 1748-3530

COVER STORY

Achieving a Stable Power Supply with Fast Transient Response Through Digital Control

Throughout the entire history of power system design there has been one requirement that has been constant: the need for a stable power supply. New trends and changing requirements in the power management industry influence how we design power supplies. Some, like the need for telemetry and system information are more recent due to advancements in technology. Others, like the demand for smaller solutions, higher levels of integration, faster transient response and high switching frequencies have been around for decades. With the introduction of Intersil's ChargeMode™ control loop technology, the ZL8800 implements a digital control topology that provides a compensation free design environment. Designed for fast transient response, the ZL8800 is able to react to a transient event in a single cycle, reducing the amount of output capacitance needed in a system. The end result is a savings in cost and board space. This article details the common problems plaguing analog voltage mode control loops and shows how a digital control loop is able to provide bandwidth that was previously dismissed as unobtainable. By walking through the variables associated with stability and comparing it to an analog control system, it can be seen that a digital control loop is able to achieve faster transient response and improved performance while maintaining a stable loop.

Full story on page 18.

Cover supplied by Intersil Corporation.

End of Exceptional Growth?

One of the major markets for high-power electronics and in particular semiconductors is not growing as fast as in the past years, it is more or less stagnating or even declining. It's the electrical drive business and thus inverters or now so-called drive controllers and thus the market for IGBT modules and DC-link components which are affected negatively. According to figures presented at the trade fair SPS/IPC/Drives (featuring 1,600 exhibitors and 60,000 visitors) in Nuremberg by the German ZVEI industry association. Jürgen Amedick, responsible for electrical drives within the ZVEI and Head of Large Drives within the Siemens Automation Group, reported a decline of more than 3 percent in turnover and production in 2013 compared to the year 2012 in Germany. "The times of record sales are over", he stated. And that is not only valid for Germany, but for Europe as a whole. And in particular, since no real investments in automation or regenerative energies can be seen in the economical struggling South European countries. This is backed by Infineon's 2013 fiscal year results - Industrial Power Control (IPC) had the most difficult year, particularly because global demand for capital goods was initially very weak. After a massive slump in the first quarter, however, the situation rapidly improved. IPC ended the 2013 fiscal year with a revenue decline of 11 percent to 651 million euros. The strong recovery of IPC continued in the fourth quarter. In comparison to the third quarter, revenue increased by 14 percent to 197 million Euros. Demand improved in all fields where IGBT chips and modules are used. Hopefully this situation will continue throughout the coming year and throughout industry.

Energy efficiency was one of the major topics at that trade fair attracting various power electronic vendors to showcase their products for high-efficient variable-speed drives, among them Amantys, Infineon, Microchip, LEM, Semikron, ST Micro and TI. Variable speed drives can save up to 30 percent of consumed electrical energy but the adoption of VSDs is slow, according to the ZVEI only each 8th drive speed is controlled effectively meaning a huge saving potential of 24 billion kWh or 3.6 billion euros. Additionally, the overall efficiency of a VSD can also be increased by using Silicon Carbide Power MOSFETs in the power stage of the drive controller. At the trade fair ST Micro announced as first European semiconductor manufacturer 1200/1700 V SiC MOSFETs featuring very low on-resistance below 100 milliohm for the 1200 V rating combined with excellent switching performance, translating into more efficient and compact systems. Compared with Silicon MOSFETs, SiC MOSFETs exhibit low on-state resistance area even at high temperatures and excellent switching performances versus the best-in-class 1200 V IGBTs in all temperature ranges, simplifying the thermal design of power electronic systems. If compared to the SiC JFET, whose complex driving stage construction required extreme care, it needed the same driving approach as a standard Si MOSFET, except for the positive 20 V to be applied to the gate, achieving at the same time a higher level of efficiency than the SiC JFET. The Si IGBT is still a valid alternative at low switching frequency of the converter, even if a lower efficiency has to be accepted by the user. On the contrary, the SiC MOSFET is able to offer similar efficiency values at frequency values that are four times higher than those of the Si IGBT. At the conference the German company Fertig Motors (a joint venture with Beckhoff Automation) introduced jointly with ST Micro a servo drive with integrated inverter based on these 1200 V SiC MOSFETs. In such applications SiC offers an additional advantage of high-temperature operation up to 200°C, whereas the switching losses are reduced by a factor of 8 and the conduction losses by a factor of 2. At nominal motor current the losses of the SiC power stage are measured at 25 W compared to 94 W with 1200 V IGBTs. Thus the new devices have proved to be more energy-efficient – but due to higher pricing adoption on a broader scale will take time. Regarding driving of these devices Infineon introduced at this fair the 1EDI compact driver which stands for robust and secure control of high-voltage power semiconductors covering all applications for power semiconductors with functional isolation. The 1EDI driver ICs are offered in eight variants that can be operated at up to voltages of 1200 V and are designed for use in applications with either IGBTs or MOSFETs. Samples of the 1EDI driver for MOSFETs and IGBTs with 6 A of output current are available now; the corresponding Evaluation Board can be ordered as of January 2014. Production start for both these variants will presumably begin in March 2014.

Next year's events such as CIPS, APEC and in particular PCIM will focus on these new opportunities offered by new technologies and devices. We will continue to inform our readers on the most recent developments and actively take part in this business by organizing a high-level panel discussion at PCIM Europe. In the meantime have a good jump into 2014.

Achim Scharf
PEE Editor

Fast-Charging Stations Set to Rise Quickly

Fast-charging technologies are driving the growth of the electric vehicle (EV) recharging market, with the cumulative number of stations established worldwide expanding by a factor of more than 100 times from 2012 to 2020, according to a new report from IHS Automotive.

Total fast-charging stations for EVs are set to reach 199,000 locations globally in 2020, up from just 1,800 in 2012. The number of these stations, meanwhile, is anticipated to rise more than threefold in 2013 to 5,900 and then nearly triple to 15,200 in 2014. Overall growth will continue at a rapid pace through 2020. "The length of time it takes to recharge an EV continues to be one of the major stumbling blocks inhibiting the widespread adoption of electric vehicles," said Alastair Hayfield, associate research director at IHS Automotive. "Compared to the time it takes to refuel an internal combustion engine vehicle, the recharge time for EVs is incredibly slow - at about four hours to charge a 24 kWh-capacity battery using a 6.6 kW on-board charger. If EV auto manufacturers could overcome this obstacle, it could lead to a high rate of adoption from environmentally minded consumers as well as those seeking to cut gasoline expenses. That's where fast charging comes in."

Hooked up to a fast-charging system, which offers a high-voltage DC charge instead of a slower AC charge, a vehicle can be fully charged in as little as 20 minutes. This could be a major step toward EVs becoming generally equivalent to ICE vehicles when it comes to refueling.

One fast-charging standard designed for electric vehicles is dubbed CHAdeMO, a primarily Japanese-backed technology. The major proponents of the technology are Japanese automotive OEMs—including Toyota, Nissan, Mitsubishi; and Japanese industrial giants—including Fuji Heavy Industries Ltd., Tokyo Electric Power Co. and more. CHAdeMO, roughly translated as "charge for moving," began deployment in 2009 in order to accelerate the adoption of electric vehicles in Japan, where EVs have found positive reception. Today there are as many as 2,445 CHAdeMO fast chargers in operation and more than 57,000 CHAdeMO-compatible EVs around the world. This accounts for as much as 80 % of all electric vehicles on the road, especially given the high concentration of EVs coming from Japan in the form of the Nissan Leaf, Mitsubishi i-MiEv, Hondo Fit EV and more. A competing solution to CHAdeMO, aptly named the combined charging system (CCS), offers electric vehicle owners the option of having a single charging inlet that can be used for all available charging methods. That includes 1-phase charging at an AC power source, high-speed AC charging with a 3-phase current connector at home or at public charging stations, DC charging at conventional household installation and DC fast charging at power-charging stations globally. CCS, which was submitted for international standardization in January of 2011, has garnered the support of Audi, BMW, Daimler, Chrysler, Ford, GM, Porsche and Volkswagen. Already BMW (i3), GM and Volkswagen (Up)

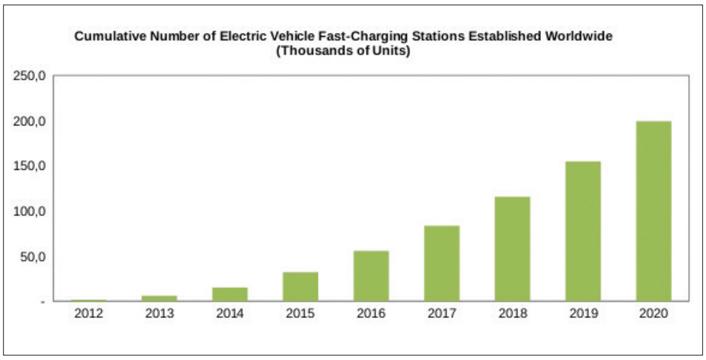

have announced they will introduce fast-charging EVs based on the CCS standard this year. Tesla Motors, the California company most notable for the all-electric Tesla Model S, is driving a third method for fast charging with its proprietary network of fast chargers in the US. Dubbed "Superchargers," the chargers operate at a higher power rating than current CHAdeMO or CCS chargers, and also have a proprietary plug interface, which means that only Tesla vehicles can use them. "In addition to the proprietary technology, the charging stations are free to use for Tesla owners, and there are plans to power all stations using photovoltaics," Hayfield said. "These Superchargers represent a powerful proposition for Tesla - drivers can charge faster, have US-wide coverage by 2015 and will charge for free for life. This triple threat will aim to lock drivers into the Tesla experience, and also will give Tesla a perceived advantage over other original equipment manufacturers competing in the same market.

Looking ahead to the future of EVs, it's clear that DC charging is becoming the favored means for supporting rapid, range-extension electric vehicles. But it is less clear as to whether CHAdeMO or CCS will win the battle for the consumer. Japan will continue to utilize CHAdeMO, while Germany is set on using CCS; other nations likely will also utilize CCS as well, since it supports slow-charging. But no matter which solution is used, DC-based fast charging is critical to promoting consumer approval and interest in Evs.

www.ihs.com

New High-Power Semiconductors Research Lab at ABB

ABB has seven Corporate Research Centers worldwide, one of them is in Baden-Dättwil, Switzerland. Approximately 220 researchers from more than 33 nations deliver leading-edge technologies and solutions in the field of power electronics and current interruption & limitation, just to mention two focus areas.

Their most recent achievement is the world's first circuit breaker for HVDC. It combines a very fast mechanics with power electronics, and will be capable of 'interrupting' power flows equivalent to the output of a large power station within 5 milliseconds. Just recently, ABB announced to invest $20 million in a new research lab for next generation high-power Silicon and wide band-gap (WBG) semiconductor devices. This investment is in conjunction with the expansion of ABB's semiconductor factories in Lenzburg, Switzerland, and Prague, Czech Republic, where in the past few years more than $200 million have been invested. Ground breaking for the new fab in Baden-Dättwil was in March 2013. The facility is planned to be in operation in summer 2014. "In the new lab power semiconductors based on Silicon, the today's standard material for high-power semiconductors, as well as on wide bandgap materials like silicon carbide will be researched. Research based on Silicon power semiconductors will be continuously transferred to Lenzburg. The research on wide bandgap materials is to demonstrate the potential of new materials," said Jan-Henning Fabian, Department Manager ABB Corporate Research.

www.abb.com/semiconductors

Chinese Inverter Manufacturer Deploys SiC MOSFETs

Shinry Technologies, a Chinese enterprise focused on energy efficient applications in transportation and lighting, employed Cree's 1200V C2M family of SiC MOSFETs in its new hybrid electric and electric vehicle (HEV/EV) power converters to achieve industry-leading efficiency. "Our customers care a great deal about efficiency, compact size and system weight and cost. The C2M

family of SiC MOSFETs allows our new HEV/EV power converters for passenger cars and busses to deliver efficiency of 96 percent in a compact size that is 25 percent smaller than current platforms", stated Wu Ren Hua, CEO of Shinry Technologies. Introduced in March 2013, the C2M family of SiC MOSFETs have been demonstrated to achieve more than three times the power density of typical Silicon technology in standard power supply designs and have been deployed in solar inverters, industrial power supplies, battery chargers, UPS and several other applications.

www.cree.com/power

Delta Electronics Deploys GaN MOSFETs in Power Supplies

Transphorm has been invited to present at Delta Electronics' exclusive Power Design Engineering event in Shanghai in November to present its 600 V GaN HEMTs and applications. Transphorm's participation as the only invited external supplier at this internal event, where Delta will share technology insights across a variety of areas at its Hangzhou Design Center (HDC) and Shanghai Design Center (SDC), will allow Delta's engineering force to proliferate the adoption of 600V GaN products in applications ranging from power supplies to various other inverters/converters.

"We have long recognized Gallium Nitride as providing unprecedented power conversion efficiency as well as reduced form factor in systems," said Dr. Alpha Zhang, Director of Delta SDC/HDC and Vice Chairman of China Power Supply Society. "Today this great promise has become a reality. With the proof that high-voltage GaN on Si is qualified and available for production, we look forward to realizing the benefits of GaN being implemented into real power products in the marketplace."

Recently Cree issued a patent license agreement with Transphorm, Inc. that provides access to Cree's extensive family of patents related to GaN high electron mobility transistor (HEMT) and GaN Schottky diode devices for use in the field of power conversion devices. The licensed family of patents addresses various aspects of making GaN power devices, including nitride materials, HEMT and Schottky diode designs and processing technology. While GaN HEMTs are already used extensively in RF markets, their use in power conversion markets has been targeted by Transphorm and a number of other companies.

www.deltaww.com, www.transphormusa.com

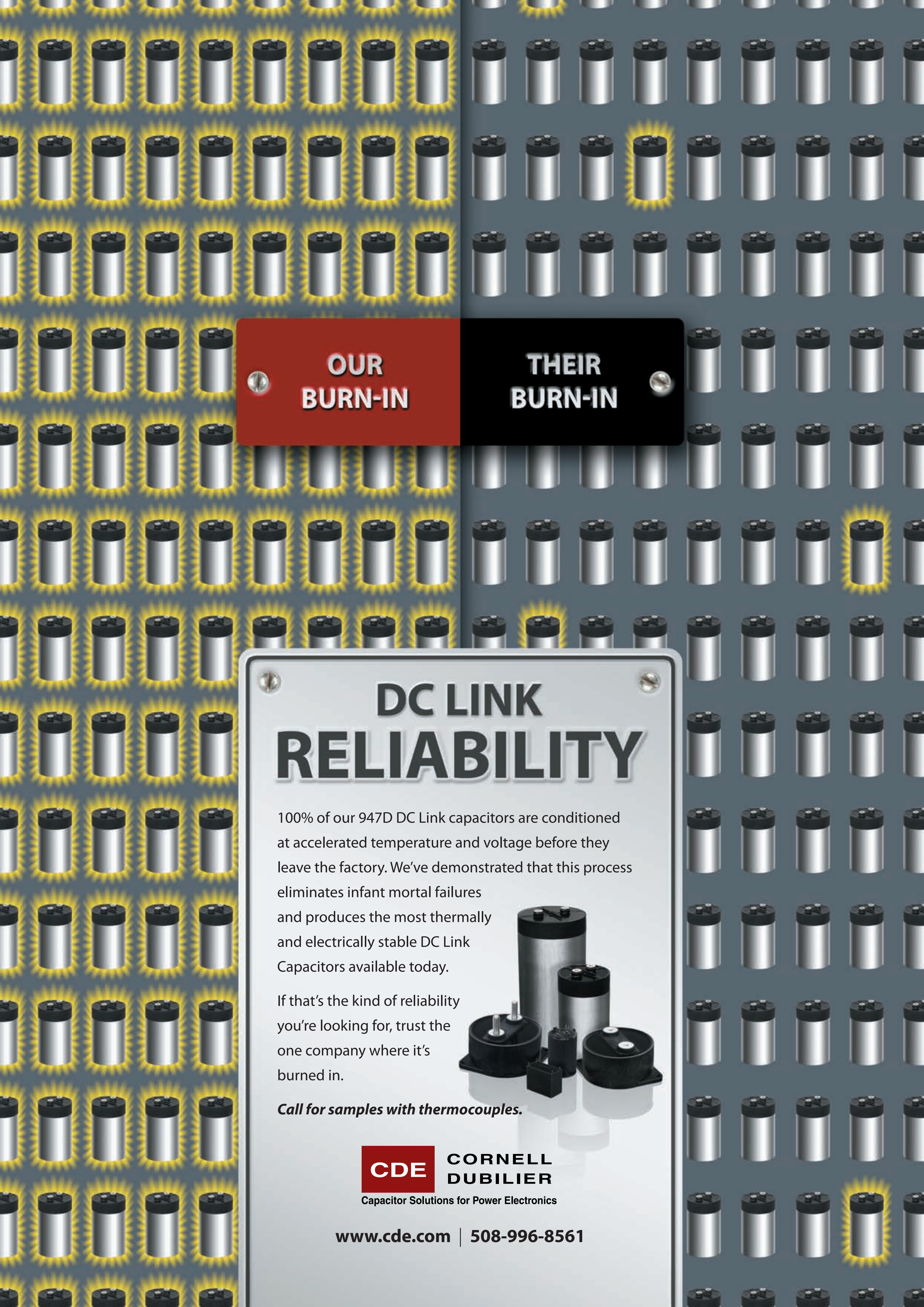
OUR BURN-IN
THEIR BURN-IN
DC LINK RELIABILITY
100% of our 947D DC Link capacitors are conditioned at accelerated temperature and voltage before they leave the factory. We've demonstrated that this process eliminates infant mortal failures and produces the most thermally and electrically stable DC Link Capacitors available today.
If that's the kind of reliability you're looking for, trust the one company where it's burned in.
Call for samples with thermocouples.
CDE CORNELL DUBILIER
Capacitor Solutions for Power Electronics
www.cde.com | 508-996-8561

RS Extends Power Portfolio

RS Components, the trading brand of Electrocomponents plc, has signed a distribution agreement with Taiwan Semiconductor on discrete semiconductor devices and power management ICs.

The Taiwan Semiconductor parts currently available to purchase direct from RS stock comprise an extensive selection of discrete semiconductors including bridge rectifiers, power Schottky and suppression (TVS), MOSFETs and small signal devices. These are complemented by a range of power management devices, which includes linear voltage regulators, switching regulators and analogue ICs. RS will continue to expand the line, introducing new products to its inventory as soon as they are released to give customers fast access to all of the latest Taiwan Semiconductor devices for use in automotive, consumer, computing, industrial, lighting, portable, power management and telecoms applications.

www.rs-components.com

Good Outlook for 2014 at Infineon

In 2013 fiscal year Infineon earned Group revenue of over 3.84 billion Euros, a decline of 2 % compared to the previous year. Beginning in the second quarter, demand recovered more dynamically than expected. Business in Asia, especially China, was especially strong.

Infineon's the three segments Automotive, Chip Card, as well as Power Management & Multimarket increased their revenue. This more than offset the decline in the Industrial Power Control segment (power modules).

Although Automotive (ATV) slowed somewhat due to the continuing weak car market in Europe, sales in the USA and China developed very well. Demand for German premium cars also remained at a high level. In a year-on-year comparison, ATV's revenue thus increased by 3 % to a good 1.7 billion Euros. But semiconductors make a substantial contribution to reducing CO_2 emissions. There is still great potential in this area, both in regard to improvements in conventional engines as well as the use of hybrid models, many more of which have been offered recently. Without the use of hybrid or purely electric vehicles, the EU limits on automobile CO_2 emissions will not be reachable. The future belongs to emission-free, fully electric vehicles. Infineon is cooperating in this area with vehicle manufacturers and partners in the supplier industry and thus contributing to optimized system solutions. One result of this cooperation the new electric BMW i3. "We are pleased that our semiconductors could contribute to a peak performance of 125 kilowatts controlled by our HybridPACK 2 IGBT power module and our 32-bit TriCoreTM microcontroller architecture. In addition, our semiconductors can be found in components such as airbag controls or the LED light module", CEO Reinhard Ploss pointed out.

Power Management & Multimarket (PMM) continued to benefit from the increasing global demand for smartphones and tablets. PMM was hardly affected at all by the decline in demand for classic PCs. Sales of high-quality laptops remained fundamentally stable compared to the rest of the PC market. With plus 6 percent to 987 million euros, PMM showed the greatest revenue increase compared to 2012. Of all the Divisions, Industrial Power Control (IPC) had the most difficult year, particularly because global demand for capital goods was initially very weak. After a massive slump in the first quarter, however, the situation rapidly improved. IPC ended the 2013 fiscal year with a revenue decline of 11 % to 651 million euros. The strong recovery of IPC continued in the fourth quarter. In comparison to the third quarter, revenue increased by 14 percent to 197 million Euros. Demand improved in all fields where IGBT chips and modules are used. "In summary, this means that in the 2013 fiscal year, our revenue and margin were better than initially expected. We played on our strengths and demonstrated outstanding management of market cycles. Even in the downturn, Infineon remained profitable", Ploss underlined. A possible Chinese competition in IGBTs through the acquisition of UK-based Dynex by a Chinese traction maker is not a problem for Ploss, the cooperation in IGBT modules with wind turbine manufacturer Goldwind works well.

As with every year, Ploss anticipates a seasonal decline in all four segments in the first quarter (October to December 2013). "The decline will probably be significantly greater in Power Management & Multimarket and Chip Card & Security than in the automotive and industrial segments. For the Group as a whole, we expect revenue between 960 million and 1 billion Euros. For the 2014 fiscal year we expect revenue growth of 7 to 11 %. In the year as a whole, we want to increase investments to circa 650 million Euros. Our changed product mix as well as the current high utilization in our production require capacity expansion in 200 mm and 300 mm thin wafers for power MOSFETs and IGBTs."

www.infineon.com

Infineon's CEO Reinhard Ploss presents the power control unit (left) for BMW's new i3 electric vehicle **Photo: AS**

ICW Announces Sales Agreement With ICEL

Wrexham-based, metallised film capacitor manufacturer ICW is pleased to announce a new joint sales agreement with and the Milan-based, film capacitor manufacturer ICEL S.R.L.

Established in 1960, ICEL manufactures a comprehensive range of box radial polypropylene and polyester capacitors for snubber, pulse power, DC link and AC filtering applications.

This new agreement means that both companies will be able to offer one another's products in their respective home markets.

David Thomson, managing director of ICW, said: "The product lines of ICW and ICEL complement one another perfectly, allowing ICW to offer a complete film capacitor solution in the UK market.

"In addition to supplying high quality, cost effective capacitors, both ICW and ICEL offer customers complete technical and development support.

"Our common approach to customers and complementary product ranges can only result in a better film capacitor solution for our customers."

A comprehensive industry cross reference to ICEL products can be found at www.icwltd.co.uk

IEDM Conference
December 9-11, 2013

Washington Hilton
Washington, DC

Tutorial Courses:
Saturday, December 7, 2013

Short Courses:
Sunday, December 8, 2013

Power Semiconductors at IEDM 2013

With a history stretching back nearly 60 years, the IEEE International Electron Devices Meeting (IEDM) in Washington/DC from December 7-11 is the world's forum for reporting technological breakthroughs in the areas of semiconductor and electronic device technology, design, manufacturing, physics, and modeling. The conference scope not only encompasses devices in Silicon, compound and organic semiconductors, but also in emerging material systems. IEDM 2013 covered also new developments in SiC and GaN.

Already on December 7 T. Paul Chow from Rensselaer Polytechnic Institute gave a tutorial on "Interface Properties for SiC and GaN MOS Devices". Wide bandgap semiconductors, such as SiC and GaN, have many attractive material properties, such as high breakdown field, which make them suitable for power electronic applications. In addition, SiC is one of the few semiconductors which can be thermally oxidized to yield a surface SiO2 gate oxide, allowing the possibility of power MOSFETs. By contrast, for GaN MOS-gated transistors, gate dielectrics, such as SiO_2, Si_3N_4 or Al_2O_3, must be deposited onto GaN.

GaN Power Transistors

An invited paper entitled "Techniques Towards GaN Power Transistors with Improved High Voltage Dynamic Switching Properties" was presented by Ferdinand-Braun-Institut, Leibniz-Institut für Höchstfrequenztechnik Berlin/Germany **(www.fbh-berlin.de)**. Current limitations of GaN power devices in terms of dynamic switching are analyzed and techniques towards improving fast high voltage switching are proposed. Normally-off and normally-on GaN transistors are presented that show a dynamic on-state resistance increase of only a factor of 2.5 after switching at 500 V drain bias. This work has been supported by the German program PowerGaNPlus and the European program HiPoSwitch.

GaN based power transistors can only gain market acceptance if they demonstrate switching properties superior to competing technologies. So far, mainly the improved static on-state resistance of these devices has been highlighted in literature, however the dynamic switching properties are often lagging behind significantly, especially at high switching voltages. This paper analyzed current

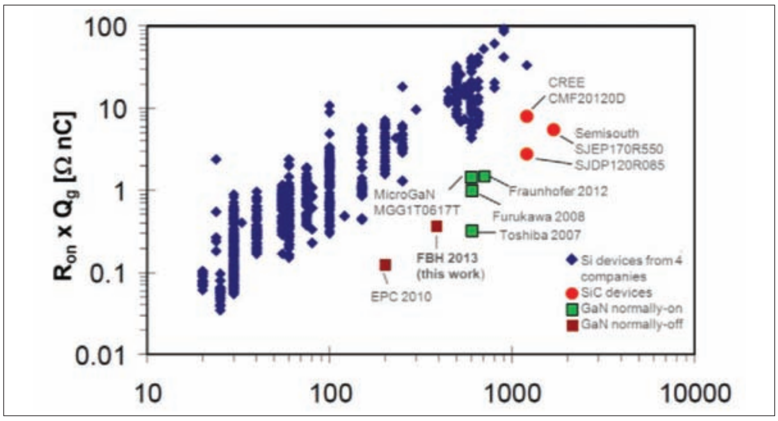

Comparison of product-specific on-state resistance and gate charge vs breakdown voltage
Source: FBH Berlin

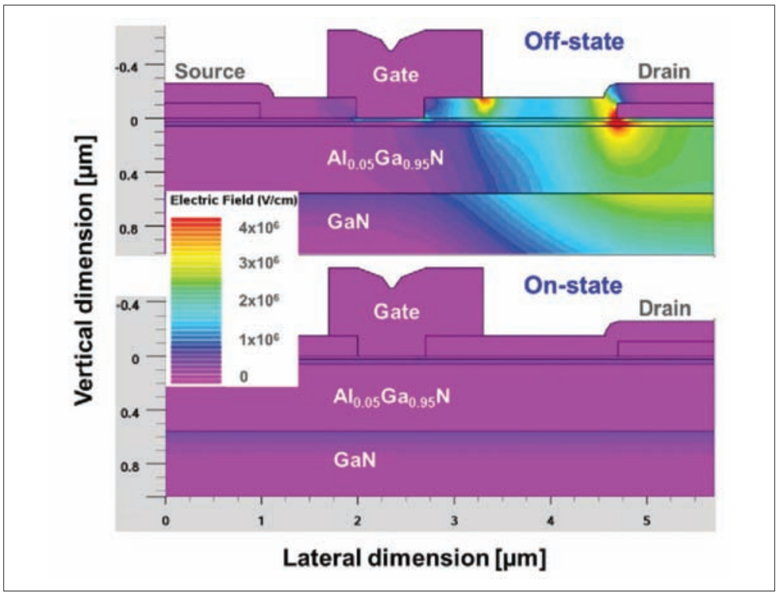

Simulation of electric field distribution at off-state (V_{ds} = 300 V) and on-state operation (V_{ds} = 1.5 V, I_d = 0.22 A/mm)
Source: FBH Berlin

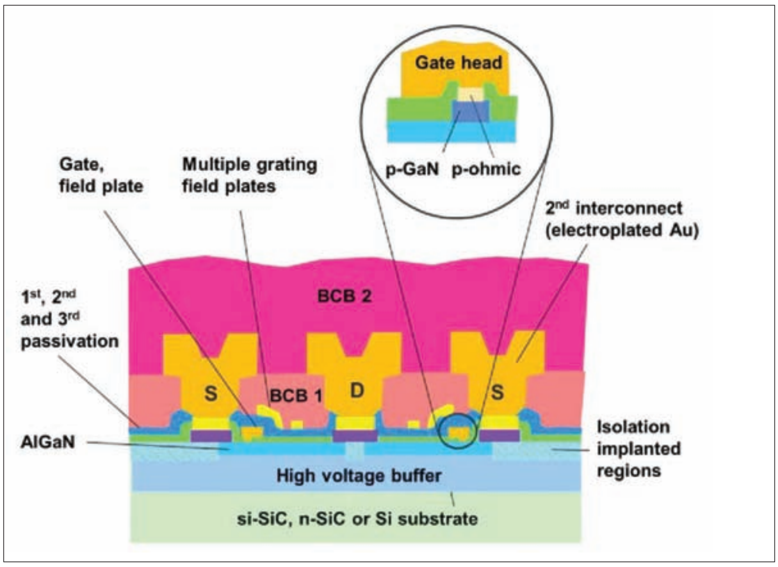

High-voltage switching GaN technology developed at Ferdinand-Braun-Institut in Berlin. Normally-on and normally-off transistors are fabricated in the same technology except the gate (insert shows details of the p-type GaN gate for normally-off operation)
Source: FBH Berlin

limitations and highlighted techniques towards improving high voltage switching properties of GaN power transistors.

The dynamic on-state resistance $R_{on\ dynamic}$ is caused by temporary charge trapping after switching, for example from off-state to on-state conditions. If negative charge trapping occurs close to the channel, electron transport in the channel region is impeded until the traps are emptied. This leads to increased switching losses. There is a tremendous advantage of GaN devices over Si devices in terms of the product "on-state resistance times gate charge" (R_{on} x Q_g). This product can be considered as a figure of merit (FOM) for switching efficiency. Therefore, any increase of R_{on} during dynamic switching reduces specific GaN advantages. The dynamic on-state resistance increases with operation voltage and can exceed the static value by more two orders of magnitude higher than the static value. Trap states in the vicinity of the channel are charging up during off-state biasing. Mostly, charging effects are related to trapping in the buffer. However, traps in the device passivation or in the AlGaN barrier layer may also be present. Simulations of electric field distribution at off- and on-state condition show remarkable differences. At off-state the electric field deeply penetrates into the semiconductor volume giving rise to charge and discharge trap states present in these regions.

Design and composition of the buffer structure significantly influences dynamic properties. Carbon acceptors in the buffer increase device (gate / drain) breakdown strength, however at the expense of an increasing $R_{on\ dynamic}$. A high breakdown strength of 120 V/µm has been obtained already a couple of years ago. However, due to the high $R_{on\ dynamic}$, these devices were not useful for switching applications. Fe doped buffer and AlGaN back barrier structures are a better choice for reducing dynamic on-resistance, but on the other hand the breakdown strength is reduced to only 40 or 50 V/µm. A good compromise can be obtained by combining AlGaN barrier and C-doping in such a way that the AlGaN barrier is placed close to the channel whereas the C-doped buffer is placed in regions underneath which are not prone to large field changes during switching. A breakdown strength of 80 V/µm and a $R_{on\ dynamic}$ increase of only a factor of 1.1 at 65 V are obtained with this combination.

With that device switching properties were significantly improved. The $R_{on\ dynamic}$ increase is limited to a factor of only 2.5 when switching at 500 V - a breakthrough showing that GaN devices really outperform Si power devices in terms of the R_{on} x Q_g product and therefore in terms of potential system efficiency. A more detailed study of the time dependency of $R_{on\ dynamic}$ unveils details of the decay. Immediately after switching from off-state, $R_{on\ dynamic}$ rapidly decreases and then flattens out without reaching its static value after 100 µs. Interestingly R_{on} does not really decrease exponentially. Moreover, measurements with higher time resolution show a decay similar to multiple exponential functions with several time constants. It is believed that this behavior relates to different trap states contributing to the charging and discharging mechanism.

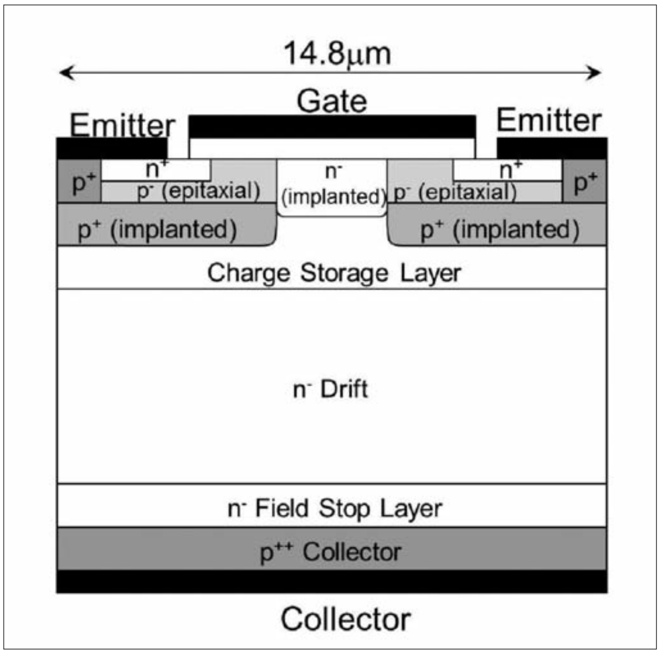

Cross-sectional view of the AIST SiC IE-IGBT Source: AIST Japan

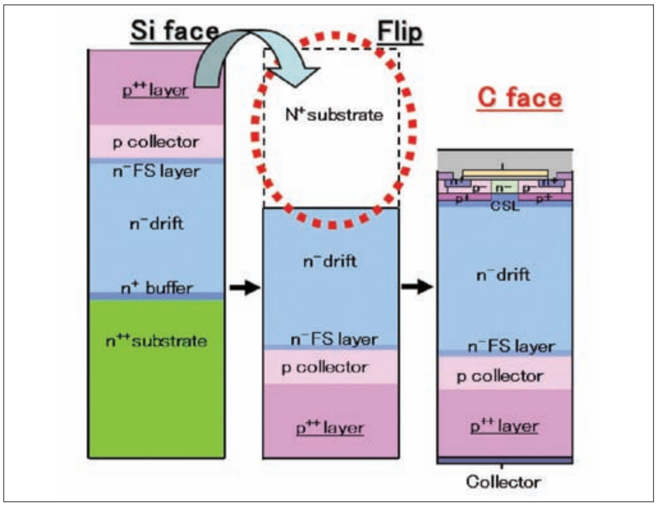

Fabrication process of the flip-type SiC IE-IGBT Source: AIST Japan

Novel SiC IGBT structure

Another invited paper "Low V_f and Highly Reliable 16 kV Ultrahigh Voltage SiC Flip-Type N-Channel Implantation and Epitaxial IGBT" by Japans National Institute of Advanced Industrial Science and Technology (AIST, **www.aist.go.jp**) presented a novel IGBT structure. SiC MOSFETs and BJTs are now very common, but IGBTs are lacking.

There is a great deal of effort under way to build "smart" power grids, with the goal of developing a more efficient and reliable electrical transmission and distribution system. The equipment used to control smart grids requires reliable, compact high-voltage switches (>10kV). IGBTs are fast, efficient high-power switches that are easy to integrate with standard CMOS circuitry. If they were made from SiC instead of bulk silicon they could handle the grid's high voltages, because SiC has 10 times the breakdown voltage of bulk silicon. The problem is, IGBT technology requires an N layer on top of a P layer, but with SiC it is difficult to grow high-quality N on top of P. This problem has been turned upside down by beginning with an N++ substrate and a high-quality N- drift layer built on top of it, and a P++ layer on top of that. Then the stack was flipped upside down and the N++ substrate was removed, which now was at the top. Once it was removed, the N- drift layer became the upper layer, atop the P++ layer. CMP was used to polish the top surface and proceeded to build the IGBT.

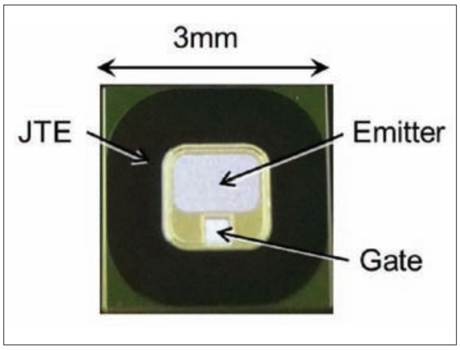

Optical microscope image of the 10 A IE-IGBT featuring 9 mm² area Source: AIST Japan

Controlling AC Motors Effectively

With the increasing demand for energy efficiency, safety, reliable connectivity and precise control, industrial drives for factory automation systems are becoming more and more sophisticated. Texas Instruments (TI) exhibited at recent SPS Drives in Nuremberg a broad range of analog products, digital controllers and software to precisely control the position, velocity and torque of mechanical drives.

The AC induction motor (ACIM) is the most popular motor used in consumer and industrial applications, and represented the "muscle" behind the industrial revolution. The concept of this "sparkless" motor was first conceived by Nicola Tesla in the late nineteenth century as a polyphase structure consisting of two stator phases in an orthogonal relationship. It has since been modified to the more common three phase structure, which results in balanced operation of the motor voltages and currents.

The motor does not have a brush/commutator structure like a brush DC motor has, which eliminates all the problems associated with

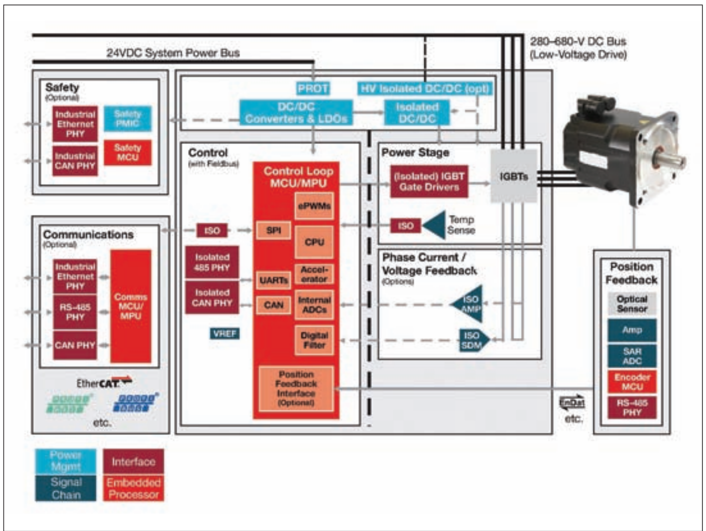

TI's offering for motor control applications

sparking; such as electrical noise, brush wear, high friction, and poor reliability. The absence of magnets in the rotor and stator structures further enhances reliability, and also makes it very economical to manufacture. In high horsepower applications (such as 500 HP and higher), the AC induction motor is one of the most efficient motors in existence, where efficiency ratings of 97 % or higher are possible. However, under light load conditions, the quadrature magnetizing current required to produce the rotor flux represents a large portion of the stator current, which results in reduced efficiency and poor Power Factor operation.

ACIMs perform best when they are driven with sinusoidal voltages and currents. One of the advantages of ACIMs is the incredibly smooth operation they can provide as a result of low torque ripple. To achieve this, most ACIMs consist of a slotted stator structure where the windings are placed in the slots with a sinusoidal winding distribution, resulting in a sinusoidal flux distribution in the airgap. This flux also links the rotor circuit, which consists of copper or aluminum bars shorted at each end, and mounted on a stacked laminate structure comprised of soft iron, or other ferrous material. In most cases, motor efficiency can be increased by decreasing the rotor bar resistance. As the flux cuts across these conductors, a d-flux/dt voltage is impressed across the rotor bars, which results in current flow in the rotor. In other words, current is induced in the rotor circuit from the stator circuit; much the same way that secondary current is induced from the primary coil in a standard transformer. This rotor current produces its own flux, which interacts with the stator to produce torque. However, in order to achieve this d-flux/dt effect on the rotor bars, the rotor cannot rotate at the same speed as the rotating stator field. As a result, induction motors are classified as asynchronous motors. The difference in rotational speed between the stator flux vector and the rotor is called slip. As more torque is required from the motor shaft, the slip frequency increases. The motor speed is a function of the number of stator poles, the motor torque (and consequently motor slip), and the frequency of the AC input voltage.

FOC basics

The three phase topology represents an ideal choice for variable-speed applications. Three phase inverters are commonly used, where motor

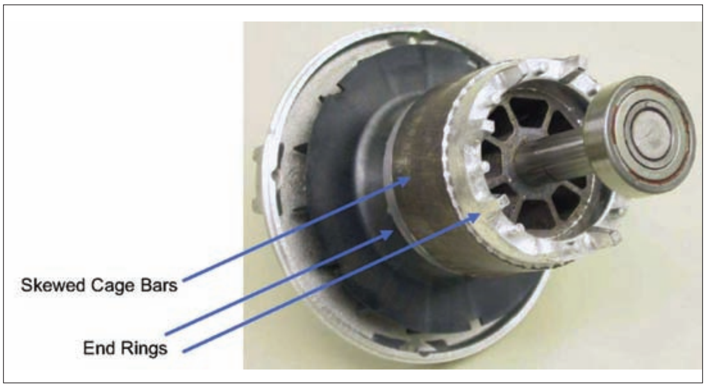

Induction motor rotor

speed can be controlled by simply varying the voltage and frequency of the applied waveform (open-loop V/Hz or scalar control). Alternately, speed can be controlled by wrapping a speed loop around a torque loop incorporating Field Oriented Control (FOC). The former can be easily achieved with an economical device such as an MSP430, but FOC is more suitable to a powerful 32-bit processor such as TI's C2000 processors.

In the V/Hz control, the speed of induction motor is controlled by the adjustable magnitude of stator voltages and frequency in such a way that the air gap flux is always maintained at the desired value at the steady-state. Sometimes this scheme is called the scalar control because it focuses only on the steady-state dynamic. It can explain how this

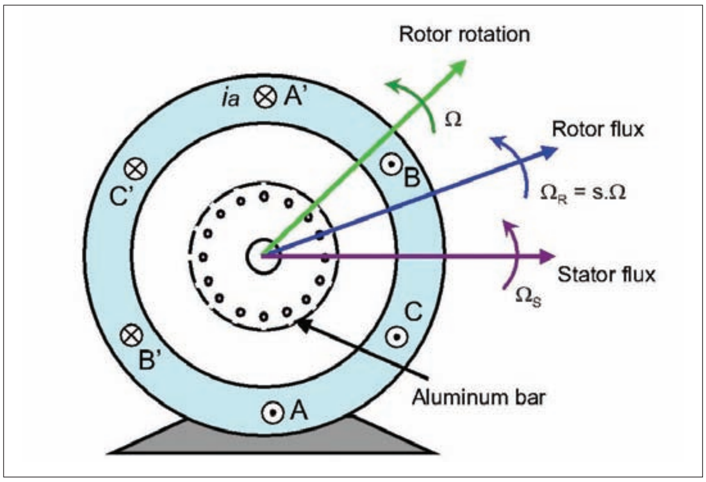

Squirrel cage rotor AC induction motor cutaway view

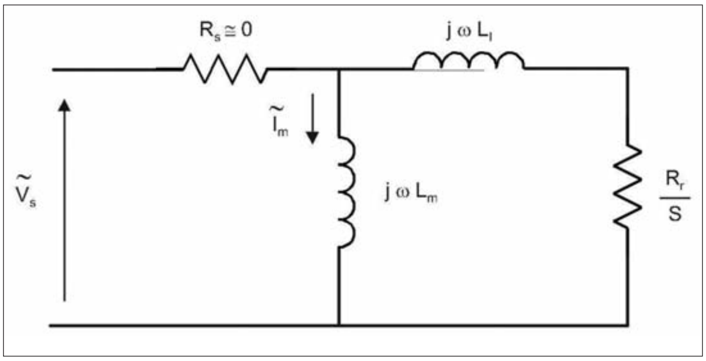

Simplified steady-state equivalent circuit of induction motor

technique works by looking at the simplified version of the steady-state equivalent circuit. The stator resistance (R_s) is assumed to be zero and the stator leakage inductance (L_{ls}) is embedded into the (referred to stator) rotor leakage inductance (L_{lr}) and the magnetizing inductance, which is representing the amount of air gap flux, is moved in front of the total leakage inductance ($L_l = L_{ls} + L_{lr}$). As a result, the magnetizing current that generates the air gap flux can be approximately the stator voltage to frequency ratio.

Microcontrollers for FOC

TI's Stellaris™ C2000™ and Hercules™ microcontroller (MCU) families are ideal for controlling an AC induction motor. All of these MCU families can be used for implementing scalar or vector-control techniques.

C2000 MCUs are designed for real-time operation and have high-resolution PWMs for precise control of gate drivers. The dual sample-and-hold, 12-bit, high-speed analog-to-digital converters (ADCs) can sample any sensor inputs with high precision. The combination of high-performance PWMs and ADCs guarantees a low torque ripple and highly efficient motor control. The C2000 MCU core architecture enables fast execution of mathematical algorithms for controlling the motors with vector control.

Stellaris MCUs are based on the widely used ARM Cortex M3 core and have all motor-control-related peripherals integrated on board. Stellaris MCUs have a 10-bit ADC and motor-control-specific PWM to provide efficient control of the motor. On-board communication peripherals such as USB and Ethernet enable the MCU to act as a networked controller that can perform motor control as well.

The RM4 and TMS570 Hercules Safety MCUs are based on the widely used ARM Cortex R4F core and are built to ease the development and certification of safety critical systems. The RM4 and TMS570 Hercules Safety MCUs have a up to 2x 12-bit ADC. The flexible HET Co-Processor delivers motor-control-specific PWM to provide efficient control of the motor. On-board communication peripherals such as USB, Ethernet and CAN enable the MCU to act as a networked controller that can perform safe motor control as well.

Isolation

TI digital isolators have logic input and output buffers separated by TI's silicon dioxide (SiO_2) isolation barrier, providing 4 kV of isolation. Used in conjunction with isolated power supplies, these devices block high voltages, isolate grounds, and prevent noise currents from entering the local ground and interfering with or damaging sensitive circuitry.

Power management

Power management IC solutions ranging from standard ICs to high-performance, plug-in, power-brick, power MOSFETs and integrated power modules. From AC/DC and DC/DC power supplies, linear regulators and non-isolated switching DC/DC regulators to PMICs and power and display solutions, power management IC solutions are available.

www.ti.com/sps2013-pr-lp-eu

Dimmable High Power LED Driver IC Family

Power Integration's new LYTSwitch-4 ICs deliver accurate output current and high efficiency for bulb and tube applications and high-bay lighting. The devices simplify design and reduce cost while ensuring that lamps deliver uniform light output and provide exceptional performance in TRIAC-dimmable applications. Even when used with leading-edge and trailing-edge TRIAC dimmers, and at low conduction angles, designs comply with NEMA SSL-7. Start-up is very fast, typically less than 500 ms, even when dimmed to less than 10% light output, and pop-on is virtually eliminated.

LED lighting is in a major growth phase driven by reduced bulb and with a delay tube cost, better performance and lifetime and last but not least consumer acceptance. Whereas in the US and parts of South America 110 VAC line voltage dominates, nearly the rest of the world relies on 220-240 VAC. This factor has to be met by LED drivers for international usage.

LYTSwitch-4 ICs feature a combined PFC and CC single-stage converter topology resulting in a power factor greater than 0.95 and efficiencies of over 90% in typical 180-240 VAC applications. Designs based on the new drivers easily meet EN61000-3-2C regulations for total harmonic distortion (THD); optimized designs deliver less than 10% THD. Regulation is better than +/- 5% across load and production spread, reducing the need for over-design to meet minimum luminance targets. The high switching frequency (132 kHz) enables smaller, lower-cost magnetics to be used, and frequency jittering reduces EMI filtering requirements. These factors enable LED-driver designs to fit easily into space-restricted bulb styles. An optocoupler or electrolytic bulk capacitors are not needed, reducing component count and increasing reliability.

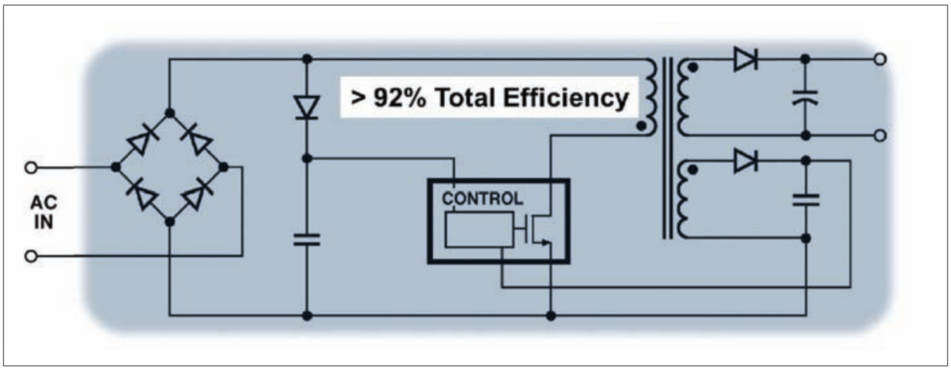

Single-stage combined PFC and CC gives highest efficiency

Continuous conduction mode flyback application

The LYTSwitch-4 high-line device (U1-LYT4324E) integrates the power FET, controller and start-up functions into a single package. Configured as part of an isolated continuous conduction mode flyback converter, U1 provides high power factor via its internal control algorithm together with the small input capacitance of the design. Continuous conduction mode operation results in reduced primary peak and RMS current. This both reduces EMI noise, allowing simpler, smaller EMI filtering components and improves efficiency. Output current regulation is maintained without the need for secondary-side sensing which eliminates current sense resistors and improves efficiency.

Fuse F1 provides protection from component failures while RV1 provides a clamp during differential line surges, keeping the peak drain voltage of U1 below the device absolute maximum rating of the internal power FET. Bridge rectifier BR1 rectifies the AC line voltage. EMI filtering is provided by L1, L2, C4, C5, R3 and R12 together with the safety rated Y class capacitor (CY1) that bridges the safety isolation barrier between primary and secondary. Resistor R3 and R12 damp any resonances formed between L1, L2, C4 and the AC line impedance. A small bulk capacitor (C5) is required to provide a low impedance path for the primary switching current. The maximum value of C4 and C5 is limited in order to maintain a power factor of greater than 0.9.

To provide peak line voltage information to U1 the incoming rectified AC peak charges C6 via D2. This is then fed into the VOLTAGE MONITOR pin of U1 as a current via R14 and R15. This sensed current is also used by the device to set the line input overvoltage protection threshold. Resistor R13 provides a discharge path for C6 with a time constant much longer than that of the rectified AC to minimize generation of line frequency ripple.

The VOLTAGE MONITOR pin current and the FEEDBACK pin current are used internally to control the average output LED current. For TRIAC phase-dimming or non-dimming applications the same value of resistance 24.9 kΩ is used on the REFERENCE pin resistor (R18) and 4 MΩ (R14 + R15) on the VOLTAGE MONITOR pin to provide a linear relationship between input voltage and the output current and maximizing the dimming range. Diode D3, VR4 and C7 clamp the drain voltage to a safe level due to the effects of leakage inductance. Diode D4 is necessary to prevent reverse current from flowing through U1 for the period of the rectified AC input voltage that the voltage across C5 falls to below the reflected output voltage (V_{OR}).

Diode D6, C9, C11, R21 and R22 create the primary bias supply from an auxiliary winding on the transformer. Capacitor C8 provides local decoupling for the BYPASS pin of U1 which is the supply pin for the internal controller. During start-up C8 is charged to ~6 V from an internal high-voltage current source tied to the device DRAIN pin. This allows the part to start switching at which point the operating supply current is provided from the bias supply via R19 and D5. Capacitor C8 also selects the output power mode (47 µF for reduced power was selected to reduce dissipation in U1 and increase efficiency).

The bias winding voltage is proportional to the output voltage (set by the turn ratio between the bias and secondary windings). This allows the output voltage to be monitored without secondary-side feedback components. Resistor R20 converts the bias voltage into a current which is fed into the FEEDBACK pin of U1.

The internal engine within LYTSwitch-4 (U1) combines the FEEDBACK pin current, the VOLTAGE MONITOR pin current and drain current information to provide a constant output current over up to 1.5 : 1 output voltage variation (LED string voltage variation of ± 25%) at a fixed line input voltage. To limit the output voltage at no-load an output overvoltage protection circuit is set by D7, C12, R24, VR2, R23, C10 and Q4. Should the output load be disconnected the bias voltage will increase until VR2 conducts, biasing Q4 to turn on via R23 and pulling down current going into the FEEDBACK pin. When the feedback current drops below 10 µA the part enters auto-restart and the switching of the MOSFET is disabled for

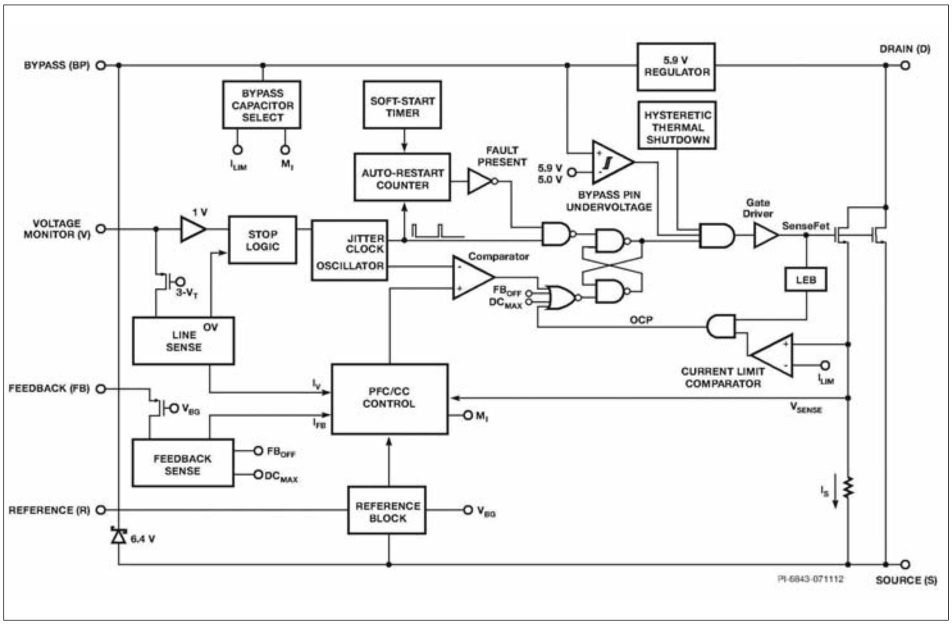

Lytswitch-4 functional block diagram

600 ms, allowing time for the output and bias voltages to fall.

The transformer secondary winding is rectified by D8 and filtered by C14 and C15. An ultrafast TO-220 diode was selected for efficiency and the combined value of C11 and C12 were selected to give peak-to-peak LED ripple current equal to 30 % of the mean value. For designs where lower ripple is desirable the output capacitance value can be increased. A small pre-load is provided by R26 which discharges residual charge in output capacitors when turned off.

The requirement to provide output dimming with low cost, TRIAC-based, leading edge phase dimmers introduces a number of trade-offs in the design. Due to the much lower power consumed by LED based lighting the current drawn by the overall lamp is below the holding current and/or latching of the TRIAC within the dimmer. This can cause undesirable behaviors such as limited dimming range and/or flickering as the TRIAC fires inconsistently. The relatively large impedance the LED lamp presents to the line allows significant ringing to occur due to the inrush current charging the input capacitance when the TRIAC turns on. This too can cause similar undesirable behavior as the ringing may cause the TRIAC current to fall to zero and turn off.

To overcome these issues two simple circuits, the MOSFET active damper and RC passive bleeder were employed. Employing these circuits however comes without penalty, since their purpose is to satisfy the holding and latching current of a TRIAC by providing some low impedance path for the TRIAC current to flow continuously during the turn-on phase will introduce additional dissipation and therefore reduced system efficiency of the supply. For non-dimming applications these circuits can simply be omitted.

More details on the device and applications under **www.powerint.com/products/lytswitch-family/lytswitch-4**

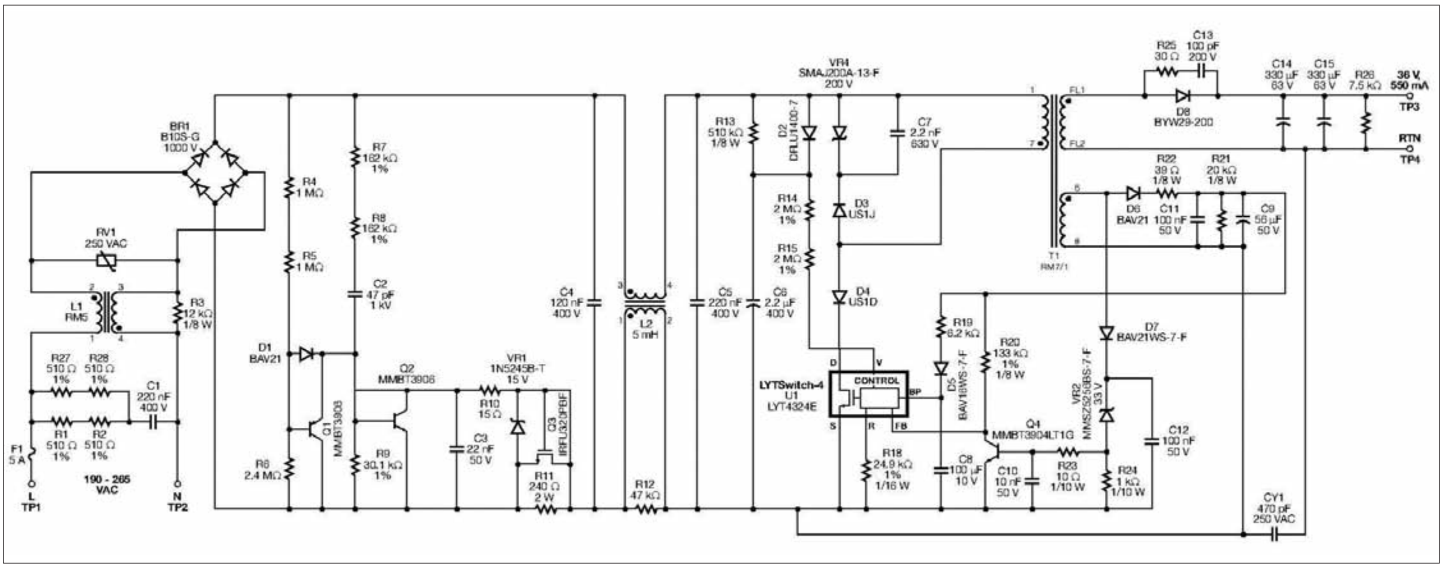

Schematic of an isolated, TRIAC dimmable, high power factor, 185 – 265 VAC, 20 W / 36 V LED driver

Achieving a Stable Power Supply with Fast Transient Response Through Digital Control

Throughout the entire history of power system design there has been one requirement that has been constant: the need for a stable power supply. With the evolution of digital control, the elusive problem of achieving power supply stability has been conquered. With the introduction of Intersil's ChargeMode™ control loop technology, the ZL8800 implements a digital control topology that provides a compensation free design environment. Designed for fast transient response, the ZL8800 is able to react to a transient event in a single cycle, reducing the amount of output capacitance needed in a system. The end result is a savings in cost and board space. **Chance Dunlap, Sr. Marketing Manager Infrastructure Power, Intersil, USA**

New trends and changing requirements in the power management industry influence how we design power supplies. Some, like the need for telemetry and system information are more recent due to advancements in technology. Others, like the demand for smaller solutions, higher levels of integration, faster transient response and high switching frequencies have been around for decades. This article details the common problems plaguing analog voltage mode control loops and shows how a digital control loop is able to provide bandwidth that was previously dismissed as unobtainable. By walking through the variables associated with stability and comparing it to an analog control system, it can be seen that a digital control loop is able to achieve faster transient response and improved performance while maintaining a stable loop.

Designing for stability

When designing point of load (POL) power supplies from a distributed rail such as +12 V, numerous options exist. The common architecture is an analog fixed frequency, voltage mode control loop with type 3 external compensation. This is popular due to the ability to adjust poles and zeroes to extend the converter bandwidth while compensating for a range of output capacitors. With a constant switching frequency the inductor and capacitor currents are predictable allowing for optimal component choice. The downside of this topology however, is the complexity of the compensation. Five external components are required which can take significant time to design. Given all the variations in the power train components it is often difficult to take full advantage of the bandwidth, the end result being a power supply with mediocre transient response. Rules of thumb suggest that a power supply bandwidth should be set in the range of 1/10 of the switching frequency (F_{sw}). But the concern is the higher that the bandwidth is pushed, the more likely the system is to suffer from pre-mature field failure. This can be seen by walking through the process of power supply design and device compensation.

When first approaching a design the common starting point is to design the power stage per the system requirements, then attempt to compensate it using resistors and capacitors in the feedback loop. The inductor and output capacitors are always sized to meet the performance specifications of the power supply, such as output current, voltage ripple, and transient performance. These components are not modified for the purposes of overall compensation as this is the responsibility of the controller or the small signal compensation components, otherwise the cost of the system could be impacted. To achieve a well compensated power supply, the expectation is that all the variables in the output filter remain constant. Unfortunately, if an analysis is performed the associated distribution of each variable can have a significant effect. For a worse case model, a Monte Carlo simulation could be run combining all the variants of L and C to create the range of transfer functions from the power stage components. Based on these results, the only potential for a stable system would be to dramatically reduce bandwidth to avoid the effect from the double pole filter.

For instance, when determining the value of L, documentation usually calls out using the nominal value that is specified on the inductor datasheet. If a worse case analysis was to be performed, this would not be adequate. Inductors have variances in inductance based on multiple factors such as inductor current, temperature, frequency and aging effects. A good example of this is when looking at non-ferrite based inductors that are popular for switch mode power supplies. Across the rated current range, the inductance can vary significantly, dropping to less than 50 % of their initial value.

Output capacitors also have wide variations in both capacitance and ESR based on operating conditions that need to be accounted for. DC bias voltages (especially with ceramic capacitors), initial tolerances, temperature, and aging effects will all change the double pole location of the output filter in the frequency domain from one board to another. With changes in DC bias and temperature, ceramic capacitors can easily drop to less than 40 % of their stated value.

From just a cursory view it can be noted that the only reliable way to compensate the device is to start decreasing the bandwidth, relying on a low frequency dominant pole to determine the bandwidth. This is in effect how internally compensated power devices are usually configured. They provide such a low bandwidth that any variation in inductance is unlikely to cause a stability problem. The downside is the restriction to use a large output capacitor to overcome the performance limitations.

This is the classic trade-off that has plagued power design engineers for years. You can optimize bandwidth at the expense of additional time calculating components, running the risk of instability due to component variation and aging. Or, utilize internal compensated devices that provide faster design time with the downside of higher BOM (bill of material) cost due to the extra capacitors required to compensate for the poor performance. The turning point to this dilemma has been the advent of digital control. By sampling the output voltage and converting it to the digital domain, advantages can be achieved through use of signal processing that would be impossible in the analog domain. The benefit of this digital signal processing is evident with the introduction of the ZL8800, a fourth generation digital controller that uses a proprietary ChargeMode control architecture to provide a compensation free solution without sacrificing performance.

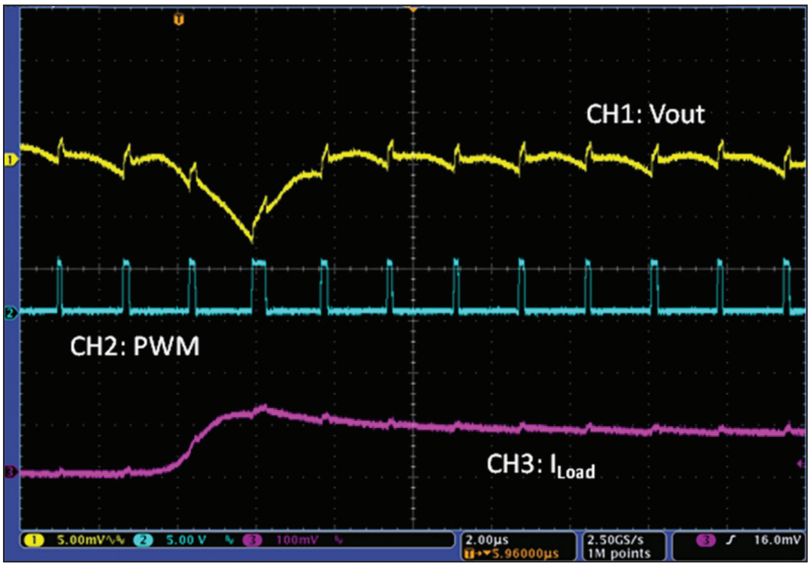

Figure 2: ZL8800 single cycle response (1 V output with 10 A load step in 1 µs)

ChargeMode controller

As can be seen in Figure 1, the ZL8800 is a dual channel PWM controller capable of converting a +12 V or +5 V to lower output voltages ideal for powering point of load applications. With a full digital control loop and internal non-volatile memory, the device eliminates the multitude of external components normally found on analog controllers. With the ChargeMode control loop technology, the burden of selecting compensation components completely disappears.

The simplification of ChargeMode control scheme is that it responds immediately to any transient event by precisely modifying the duty cycle so that the amount of charge lost on the output capacitor can be replaced in a single cycle. This is achieved by over sampling the output voltage so that corrections can be made without having to know the actual capacitor value. The benefit of the non-linear response is that a load transient can be responded to and possibly corrected in one cycle with minimal ringing or overshoot. Comparatively in analog systems the ability to react quickly usually results in an under-damped system with low phase margin risking instability and excessive ringing.

An example of the ZL8800's ability to respond to a transient event is shown in Figure 2. In this situation a 10 A load step is applied with a slew rate of 10 A/µs.

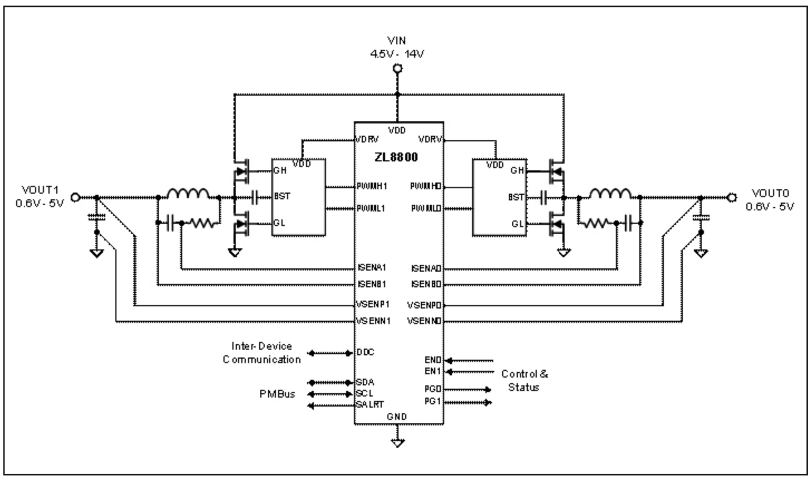

Figure 1: Typical application diagram of ZL8800

The ability to respond to a transient response at this speed sets the ZL8800 apart from other power controllers. But the real ability lies in the fact that this is achieved without compensation. In addition to the high speed loop, the ZL8800 ChargeMode control architecture is inherently stable. This means that any combination of inductance and output capacitance can be applied and the loop will remain stable. By designing a digital architecture that enforces system stability, any effect on the outside circuit such as removing capacitors dynamically or aging/thermal effects will not cause a problem.

One of the other benefits of the control loop is the ability to extend the bandwidth up to and beyond $F_{sw}/4$. The ability to achieve this is due to several approaches taken in the device. The first is a double edge modulation technique allowing the PWM signal to have a fixed frequency, but modulate both edges providing double the sampling rate in the system. Combined with a high speed ADC over-sampling the output, a wide bandwidth can be achieved without the high frequency phase roll-off common in other converters. As a result, when the bandwidth is increased the phase margin will remain stable.

Adjustable feedback gain

To allow the designer a degree of freedom in selecting the bandwidth, the ZL8800 incorporates a feedback gain term that can be adjusted to increase the response. The default gain of 256 provides a stable setting that will provide a bandwidth equivalent to an analog product that has been nominally compensated. Increasing the gain (typical range of 100 to 1200) allows a designer to dial in a faster

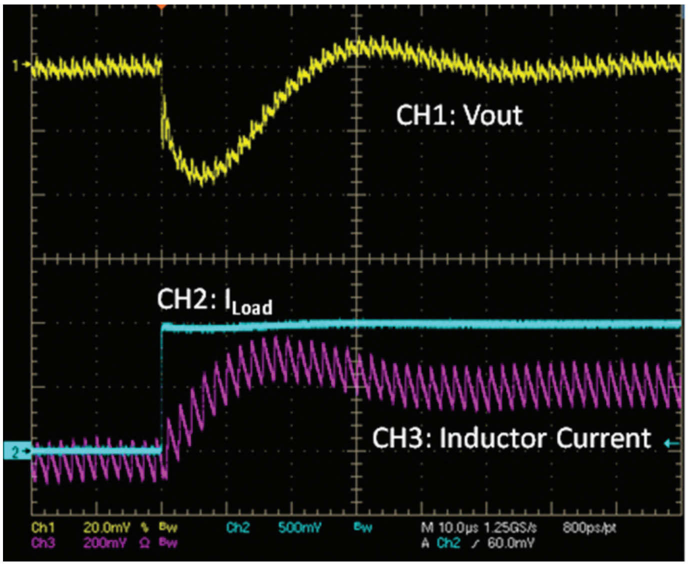

Figure 3: Transient response with gain setting = 250 (bandwith = 26 kHz)

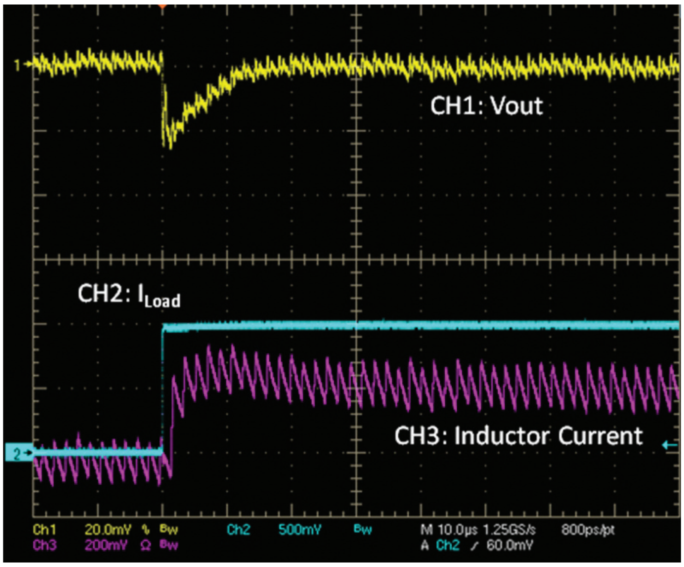

Figure 4: Transient response with gain setting = 650 (bandwith = 70 kHz)

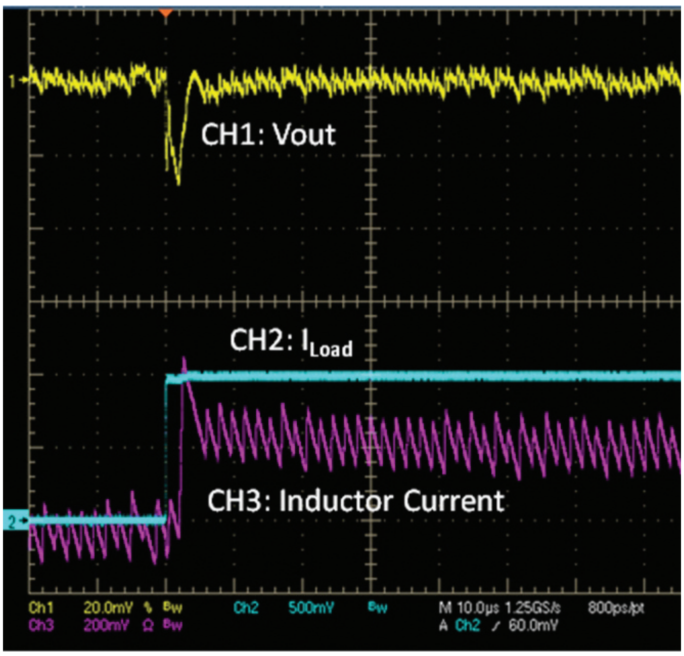

Figure 5: Transient response with gain setting = 1050 (bandwith = 140 kHz)

response with an associated trade-off of higher jitter in the PWM signal. With typical systems employing low ESR capacitors, any increase in jitter has minimal effect, hence the recommendation is always to optimize for transient response.

The scope shots shown in Figures 3, 4 and 5 illustrate how increasing the gain of the ZL8800 can result in higher bandwidth and improved transient response. In all cases, the same control loop algorithm is applied, maintaining a stable system without the need for compensation. The scope shots were taken with a board under the following conditions:

- V_{in} = 12 V
- V_{out} = 1V
- C_{out} = 1500 µF
- Inductor = 300 nH
- F_{sw} = 550 kHz
- 10 A load transient applied at 100 A/µs.

Figure 3 shows the ZL8800 transient response while running with the feedback gain set to 250. When the loop gain was measured, this equated to a loop bandwidth of 26 kHz. Increasing the gain to 650 resulted in a faster transient response with improved settling time. This can be seen in Figure 4. With this setting, the equivalent loop bandwidth was 70 kHz. Increasing the gain further to 1,050 provided even faster response, allowing the loop to compensate in almost a single cycle. As can be seen in Figure 5 the inductor current slews up to the optimal point allowing the output voltage to immediately recover without overshoot or ringing. In this situation the loop bandwidth was 140 kHz which corresponds to just over 25 % of the switching frequency.

Conclusions

In conclusion, it can be seen that power converters relying on analog compensation techniques have limitations in providing high bandwidth designs without compromising stability or long term reliability due to component variation and aging. With the ZL8800 digital control architecture it is possible to design a power converter that is compensation free with high bandwidth. These capabilities allows for a power supply to be developed in a short period of time while saving on output capacitance.

ZL8800 Digital DC/DC Power Controller

Base-stations, routers, and similar infrastructure designs require fully control and monitoring of every power rail in order to maximize reliability, and typically use monitors and sequencers to provide added functionality around the POL converters. The ZL8800 integrates all of these functions, so a designer can monitor and control every aspect of the power supply through a PMBus™ interface, without the need for additional parts. Telemetric data is available on the power supply, including temperature, input current, output current, input voltage, output voltage and fault status.

Each ZL8800 output can operate independently or together in a dual phase configuration for high current applications. The device supports a wide range of output voltages (0.54 V to 5.5 V) operating from input voltages from 4.5 V up to 14 V. The ZL8800 is available in a 7 x 7 44-pin QFN package with prices starting at $4.90 each, in 1,000-piece units. There are also two evaluation kits available, the ZL8800-2CH-DEMO1Z 2-output demo board, and the ZL8800-2PH-DEMO1Z, a 60 A 2-phase demo board. Both are available for $150.00 each.

Intersil also announced a new version of its PowerNavigator™ graphical user interface, enabling designers to leverage all the capabilities of the ZL8800 digital controller without writing a line of code. Designers can use the drag-and-drop utility to set up and control any power supply architecture, further simplifying the development effort.

Equivalent Capacitance and ESR of Paralleled Capacitors

Parallel connection of capacitors is widely used in power electronics to decrease high frequency ripples and current stress, to decrease power dissipation and operating temperature, to shape frequency response, and to boost reliability. **Alexander Asinovski, Principal Engineer, Murata Power Solutions, Mansfield, USA**

Parallel connection of capacitors is widely used in power electronics to decrease high frequency ripples and current stress, to decrease power dissipation and operating temperature, to shape frequency response, and to boost reliability. Main questions a designer faces with regard to the parallel connection of capacitors are: What are equivalent capacitance and ESR (electric series resistance) values? What is high frequency ripple voltage? What are individual RMS currents?

If all capacitors in the parallel connection are identical with equal capacitance values, $C_{sk} = C$, $k = 1,2...N$ and equal ESR values $R_{sk} = R_s$ the answers are obvious: C_{se} is directly proportional to the number of capacitors N, $C_{se} = NC$, R_{se} is inversely proportional to N: $R_{se} = R_s / N$, ripple voltage V (RMS value) for a sinusoidal current excitation $i(t) = I\sqrt{2}\sin(2\pi ft)$ with frequency f, and RMS value I is

$$V = I\sqrt{R_{se}^2 + X_{se}^2}\ , \qquad (1)$$

where $X_{se} = 1/(2\pi fC_{se})$is the reactance of the equivalent capacitor C_{se} and individual RMS currents in the capacitors are identical: $I_k = I / N$.

In case capacitors in the parallel connection are not identical, with different capacitance C_{sk} and ESR R_{sk} values, the solution to the problem is not trivial. The direct approach would be obtaining an analytical expression for the input impedance of the parallel connection in the algebraic form $Z = \mathrm{Re}Z - j\,\mathrm{Im}\,Z$ and using the formulas $R_{se} = \mathrm{Re}Z$, $X_{se} = \mathrm{Im}\,Z$ and $C_{se} = 1/(2\pi fX_{se})$. A less complicated approach taken below is based on the conversion of series, C_{sk} , R_{sk} connections to equivalent parallel C_{pk} , R_{pk} connections. To obtain relationships between R_{pk} and R_{sk} , and also between C_{pk} and C_{sk} , set admittance Y_{pk} of the parallel C_{pk} , R_{pk} and admittance Y_{sk} of the series C_{sk} , R_{sk} connections equal to each other: $Y_{pk} = Y_{sk}$, $\mathrm{Re}(Y_{pk}) = \mathrm{RE}(Y_{sk})$ and $\mathrm{Im}(Y_{pk}) = \mathrm{Im}(Y_{sk})$. It follows:

$$C_{pk} = C_{sk} / \left[1+\left(R_{sk} / X_{sk}\right)^2\right], \qquad (2)$$

$$R_{pk} = \left(R_{sk}^2 + X_{sk}^2\right) / R_{sk}\ , \qquad (3)$$

where

$X_{sk} = 1/2(2\pi\ fC_{sk})$ (4)

is the reactance of the individual capacitor.

After individual parallel capacitance C_{pk} and resistance R_{pk} values are calculated according to (2) and (3), equivalent parallel capacitance C_{pe} can be easily found as the sum of C_{pk}

$$C_{pe} = \sum_{k=1}^{N} C_{pk} \qquad (5)$$

and real part of equivalent admittance can be found as the sum of admittances $1/R_{pk}$. R_{pe} can be obtained as a reverse value of that sum:

$$R_{pe} = 1/\left[\sum_{k=1}^{N}\left(1/R_{pk}\right)\right]. \qquad (6)$$

Equivalent series capacitance C_{se} and ESR R_{se} of the system can be found by conversion of the parallel C_{pe} , R_{pe} connection to the equivalent series connection C_{se} , R_{se}. To obtain relationships between C_{se} and C_{pe} and also between R_{se} and R_{pe} , set impedance Z_{pe} of the parallel C_{pe} , R_{pe} and impedance Z_{se} of the series C_{se} , R_{se} connections equal to each other: $Z_{pe} = Z_{se}$, $\mathrm{Re}\,Z_{pe} = \mathrm{Re}\,Z_{se}$ and $\mathrm{Im}\,Z_{pe} = \mathrm{Im}\,Z_{se}$. It follows:

$$C_{se} = C_{pe}\left[1+\left(X_{pe} / R_{pe}\right)^2\right], \qquad (7)$$

$$R_{se} = R_{pe} / \left[1+\left(R_{pe} / X_{pe}\right)^2\right], \qquad (8)$$

where

$$X_{pe} = 1/\left(2\pi fC_{pe}\right) \qquad (9)$$

is reactance of the equivalent parallel capacitor C_{pe} (5).

Based on the analysis presented above, calculation procedure for equivalent series capacitance, ESR, voltage ripples , and RMS currents in the capacitors is as follows:

1. Calculate reactances of individual capacitances according to formula (4).
2. Determine equivalent parallel parameters C_{pk} , R_{pk} of the capacitors based on equations (2) and (3).
3. Calculate equivalent parallel capacitance C_{pe} of the structure, its reactance X_{pe} , and equivalent parallel resistance R_{pe} according to formulas (5), (9), and (6).
4. Calculate equivalent series capacitance C_{se} and ESR R_{se} of the structure according to formulas (7) and (8).
5. Obtain RMS ripple voltage V using equation (1).
6. Calculate RMS currents I_k in the capacitors based on the formula

$$I_k = V / \sqrt{{R_{sk}}^2 + {X_{sk}}^2}\ . \qquad (10)$$

It is worthwhile to note that ESR values are strong functions of frequency. A designer should use ESR data specified by capacitor manufacturers at a given frequency of operation. An example of a comprehensive source of data for ceramic and polymer aluminum electrolytic capacitors is found on the Murata Manufacturing Co., Ltd. (MMC) website http://ds.murata.co.jp/software/simsurfing/en-us/index.html.

To illustrate the calculation procedure let's determine equivalent parameters, voltage ripple, and current distribution for a parallel connection at of three ceramic capacitors GRM21BR60J226ME39L and one polymer capacitor ESASD40J107M015K00 from MMC.

Assuming the following input data: $f = 200$ kHz , $C_{s1} = C_{s2} = C_{s3} = 22\mu$F, $R_{s1} = R_{s2} = R_{s3} = 4m\Omega$ $C_{s4} = 100\mu$F, $R_{s4} = 8$mΩ, I = 2A.

1. For reactance of each individual capacitance according to formula (4) we have: $X_{s1} = X_{s2} = X_{s3} = 3.6\ m\Omega$, $X_{s4} = 0.8m\Omega$.
2. Equivalent parallel parameters C_{pk} , R_{pk} of the capacitors based on formulas (2) and (3) are: $C_{p1} = C_{p2} = C_{p3} = 21.7\ \mu F$, $R_{p1} = R_{p2} = R_{p3} = 331\ m\Omega$, $C_{p4} = 49.7\ \mu F$, $R_{p4} = 16m\Omega$.
3. For equivalent parallel capacitance C_{pe} , its reactance X_{pe} , and equivalent parallel resistance R_{pe} of the structure according to formulas (5), (9), and (6) we calculate: $C_{pe} = 115\mu F$, $X_{pe} = 6.9\ m\Omega$, $R_{pe} = 13.9\ m\Omega$.
4. Equivalent series capacitance C_{se} and ESR R_{se} according to formulas (7) and (8) are: $C_{se} = 143.4\mu F$, $R_{se} = 2.76m\Omega$.
5. For RMS ripple voltage based on equation (1) we obtain: $V = 12.4$ mV.
6. RMS currents according to formula (10) in ceramic and polymer capacitors are respectively: $I_1 = I_2 = I_3 = 341mA$, $I_4 = 1.1A$.

Optimized Design for Vibration Resistant Power Module Package

IGBT based power modules designed for typical industrial applications cannot be transferred to Commercial, Agriculture and Construction Vehicles (CAV) applications without changes. This article describes the simulation flow to construct a more vibration resistant power module for CAV applications. Vibration simulation (modal and harmonic analysis) is a faster and more effective method for the optimization of a design concept rather than hit and miss trials. **Frank Sauerland, Infineon Technologies AG, Warstein, Germany**

Optimization of the package begins with the evaluation of mechanical behavior under a set of vibrational load characteristics (such as vibrational harshness [1-3]) for the new applications. Designs which meet the vibration criteria were further analyzed for suitable thermal behavior. This design flow leads to a thermally feasible and mechanically optimized component for CAV applications. In particular the potential of case specific design optimizations based on simulation, using an example of a bus bar in an IGBT based power module has been evaluated. The overall goal of the optimization was to design a module and its components that comply with the higher vibration requirement for CAV applications. The enclosure body and effectively the bus bars have to perform in a harsh vibration environment.

Vibration tests shows that a power module which is constructed for industrial systems satisfies the requirements for vibration resistance in a typical application but not the higher requirements for the CAV applications (Figure 1). In order to check the vibrational resistance of a power module for an industry application the module was shaken with 5 g force between 5-150 Hz. The module passed the test since no damage was found. The power module for a CAV was shaken with an increased 15 g force vibration profile between 5 Hz until 2000 Hz [4].

Optimization of vibration resistance

For a better understanding of the vibration resistance and the failure mode of the bus bars, the module can be simplified in the following way (Figure 2 left). The power module (Figure 2 right) consists of three bus bars which can be simplified as three springs and the plastic housing which can also be simplified as a spring. The springs are connected with the base plate on the one end and on the other end with a mass. Optimization of the vibration resistance involves increasing the elastic force of the housing and lowering the elastic force of the bus bars. The elastic force of the bus bar can be reduced by lengthening the feet. The elastic force of the housing can be increased by adding reinforcements.

Frequency or modal analysis

Simulation of the modal analysis is a good aid to find the resonance frequency and to detect the weak spots of the module. The next picture shows the results of modal analysis and shows the first harmonic vibration. Figure 3A shows the deformation of the bus bars in the power module, Figure 3B shows the deformation of the housing during the first resonance frequency. Both simulations show that the critical points can be found in the housing and at the feet of the bus bars.

The simulation confirms the result from the vibration tests. For further improvement of the model with longer feet and a reinforced housing design, it is necessary to perform a frequency analysis.

The comparison of the new constructed bus bars with the conventional design

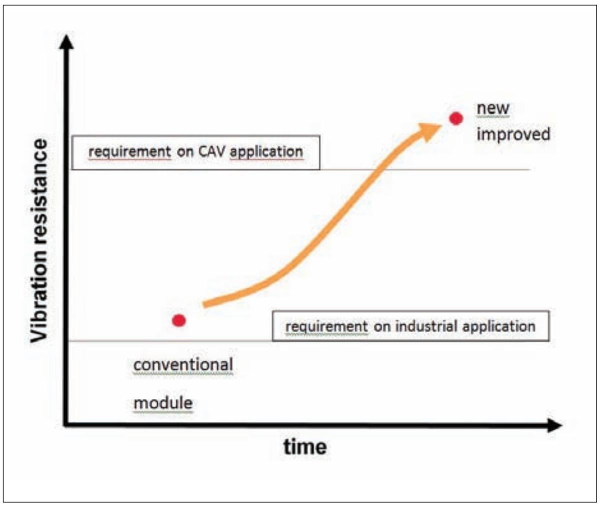

RIGHT Figure 1: Vibration resistance of the conventional and new power module

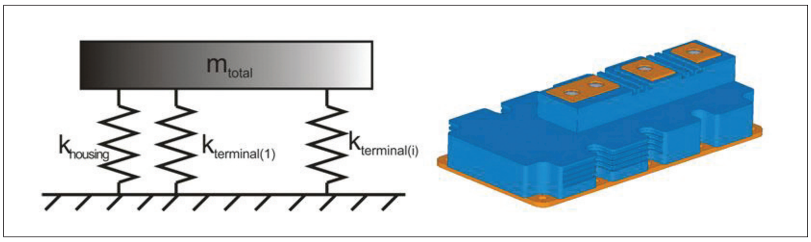

BELOW Figure 2: Model to simplify the module construction

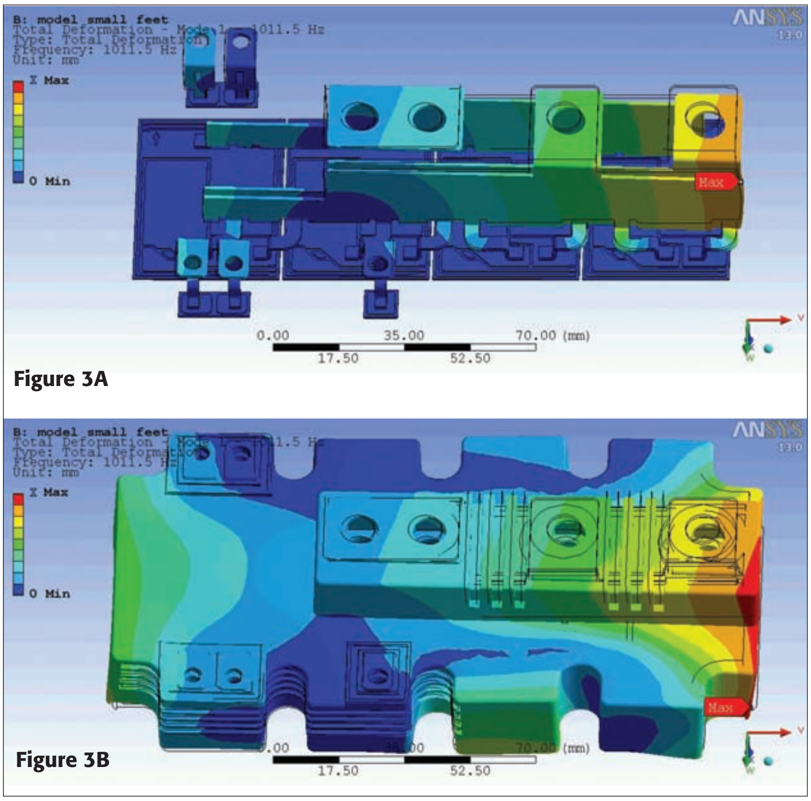

Figure 3: **Result of the modal analysis at the first resonance frequency**

under the same harmonic vibration shows a lower stress than in the new bus bars. Figure 4A shows the result of the frequency analysis of the module with the short feet, Figure 4B shows the result of the module with the long feet. The maximum stress produced in the feet of the old module was three times greater than in the new one. In the new and in the old modules the maximum stress was found to be in the same place.

The simulation is a faster alternative to producing and measuring the new bus bars and was equally effective in finding a solution.

Boundary conditions of electro-thermal analysis

The bus bar now must be tested for the electro-thermal properties.

For the power module it is very important that during operation the temperature does not exceed the highest value allowed. The improvement of the mechanical behavior of the bus bars cannot be done at the cost of the thermo-electrical behavior. Therefore the current carrying capability of the new design has to be investigated. An optimization procedure is done to investigate thermo-electrical and vibration behavior.

Figure 5 shows the circuit diagram of the half bridge and the three bus bars. The plus and the minus bus bars can be loaded with a maximum current of $I_{C\ nom}$ /4 x 20,5 per foot. The maximum allowed current for this application is IC nom with an effective value of $I_{C\ nom}$ / 20,5. In the AC bus bar the full current that flows through each foot is $I_{C\ nom}$ /4.

Application relevant thermal boundary conditions were considered for the electro-thermal simulation. The contact between the bus bar feet and the copper substrate of the DCB is fixed at a temperature and the areas of the connecting points also have a constant temperature.

Result of the electro-thermal simulation

After determination of the overall conditions the simulation can be started. The temperature distribution of the three bus bars is illustrated in Figure 6. It shows that the maximum temperature in the bus bar is lower than the maximum specified temperature. Hence the simulation shows that the new bus bar fulfills the thermal requirements as well.

The simulation results show the final compliance of the design changes in both thermal-electrical and frequency analysis. As an example of the simulation flow, every design change of the bus bar requires this simulation cycle to be redone until the results are acceptable. Even with multiple iterations, simulation is a way to evaluate the optimization concepts faster and for less cost than by producing and measuring all possible designs.

Conclusions

It was explained that the virtual investigation of a bus bar design alternatives using simulation is faster than other techniques such as hit and miss

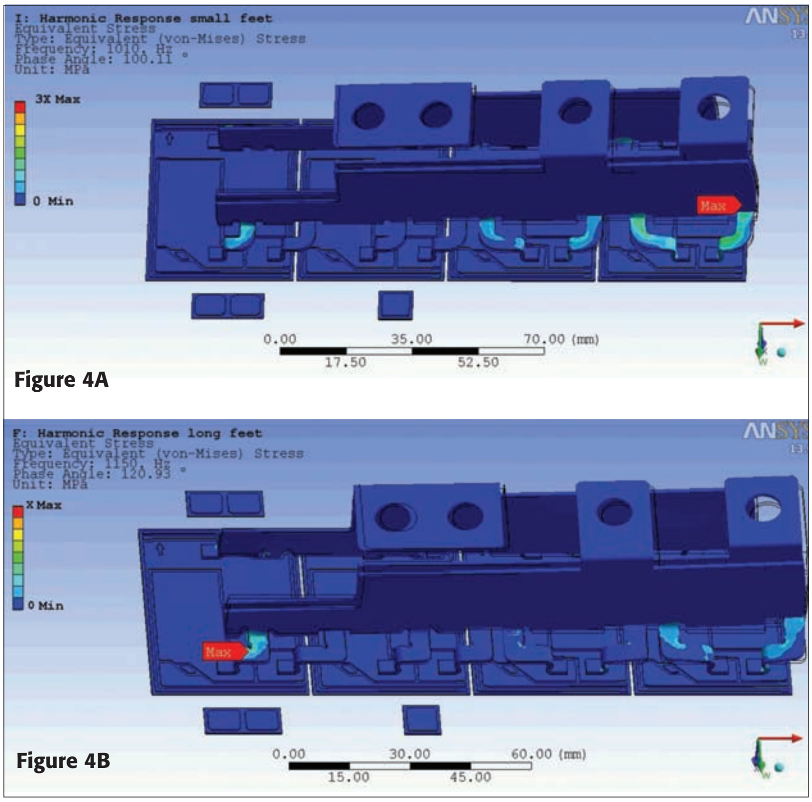

Figure 4: **Figure 4A shows the result of the bus bar with small feet, Figure 4B the result for the long feet**

RIGHT Figure 5: Circuit diagram of the half bridge and the three bus bars

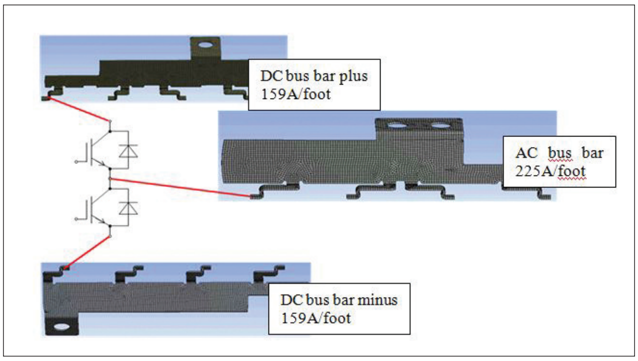

BELOW Figure 6: Temperature distribution in the bus bars under electro-thermal loadings

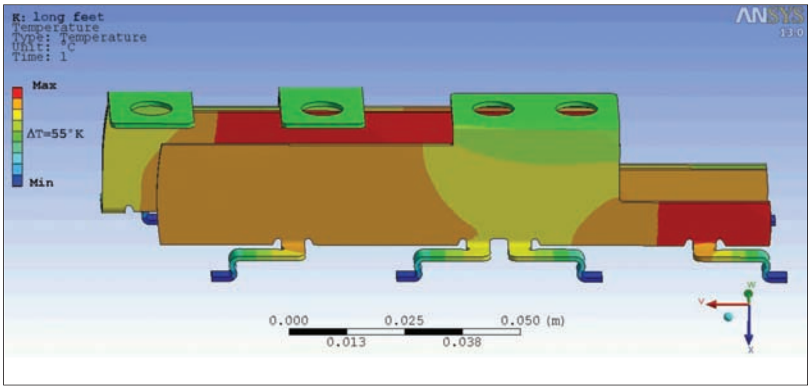

trials. Modal analysis using simulation is seen to be a very good instrument to find the critical points of the design. Harmonic analysis calculated the stress level to compare different designs. After mechanical optimization, the improved design is investigated by the thermal-electrical simulation, which provides the thermal state at maximum current.

Literature

[1] Piotr Luniewski, Michael Sleven, Krzysztof Mainka, Dave Levett, "The Technical Benefits of PrimePACK™ Modules in CAV Applications", May 2009

[2] M. Thoben, „Abschlussbericht Elektrokomponenten für Aktivgetriebe: Hochtemperaturtaugliche Verbindungstechnik, Stromsensorik, Treiber-IC zur Getriebeintegration der Leistungselektronik und Ankopplung an den Kühlkreislauf des Verbrennungsmotor", FKZ 19U6006C, 2011

[3] Teil 2-6: Prüfverfahren – Prüfung Fc: Schwingen (sinusförmig) IEC 60068-2-6

[4] Guido Strotmann, Georg Borghoff, Christoph Pannemann, Andreas Vetter „Ultraschallschweißen: Zuverlässige Hochstromverbindungen für hohe Temperaturen", 36. Kolloquium „Halbleiter-Leistungsbauelemente und ihre systemtechnische Anwendung", Nürnberg

Quality Test Systems for High-Power Semiconductors

With more than 30 years of experience, ABB designs and manufactures CE compliant customized test systems, covering the entire range of high-power semiconductor testing capabilities. Presently, over 70 test systems are in operation for routine and reliability measurement of power semiconductors, some of them have been in operation for more than 15 years. Thanks to close proximity to semiconductor development, application and production, we are in an ideal position to provide measurement systems to meet customers' needs. Automation, safety, operator friendly handling and easy to maintain are among the designed-in features. **R. Leutwyler, S. Gekenidis, ABB Switzerland Ltd, Semiconductors, Lenzburg, Switzerland**

Customers expect high-power semiconductors to be extremely reliable and without any failures while still being inexpensive. Continuous product quality improvement and production efficiency enhancement are therefore among the main focus areas of high-power semiconductor manufacturers. Taking advantage of customized and highly automated test systems is one answer to this challenge.

ABOVE Figure 1: Static and dynamic test system for thyristors and diodes

Electrical test system

There is a broad variety of high-power semiconductor devices like diodes, phase control thyristors (PCTs), bi-directionally controlled thyristors (BCTs), fast switching and reverse conducting thyristors, gate turn-off thyristors (GTOs), integrated gate-commutated thyristors (IGCTs) or insulated gate bipolar transistors (IGBTs) available on the market. Their current and voltage ratings range from several hundred to about 5,000 A and from slightly above thousand to more than 8,000 V. These devices must be tested and characterized, however, at currents and voltages of up to 10 kA and 14 kV, respectively. Prior to shipment high-power semiconductors are tested statically and dynamically, at hot and cold temperatures and also undergo single-pulse and multi-pulse tests.

While production test systems are optimized for high throughput and the measurement of a fixed set of parameters of finished devices, test systems used in R&Dor in failure analysis labs must assure a high degree of flexibility to easily adapt to different voltage and current ranges, electrical configurations and mechanical footprints of subsystems, subassemblies or even wafers or chips.

It goes without saying that state-of-the art high-power semiconductor test systems must assure accurate, repeatable, reliable and save measurements and comply with internationals standards.

An example of a static and dynamic PCT and diode production test system is shown in Figure 1. This test system features an electrical breaker to protect the test system

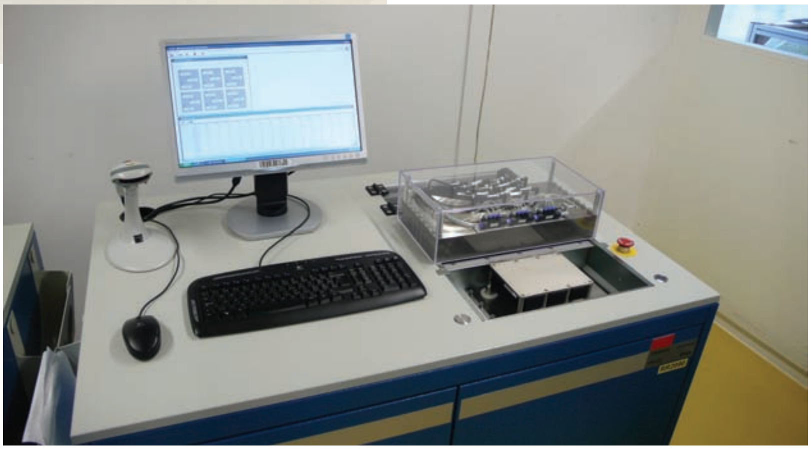

Figure 2: Baseplate flatness test system

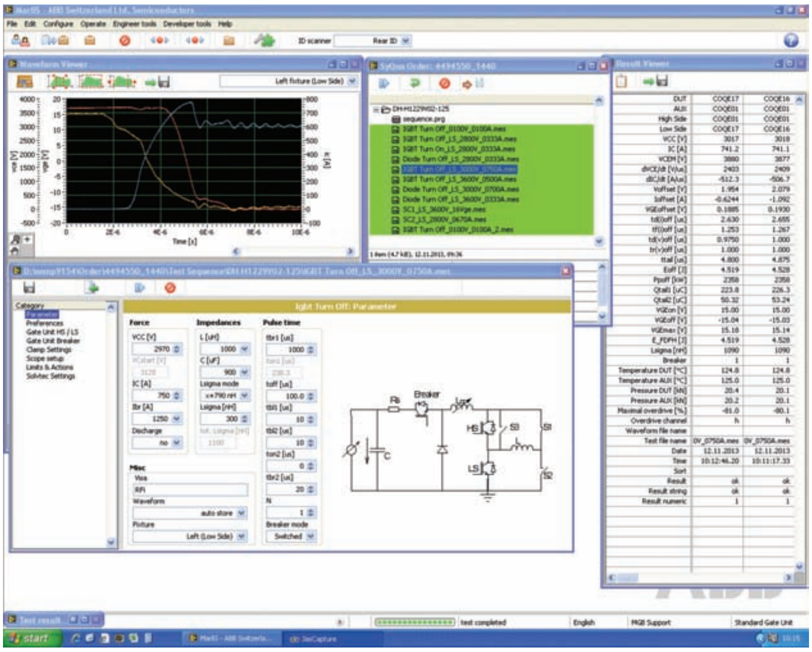

Figure 3: Typical main user interfaces

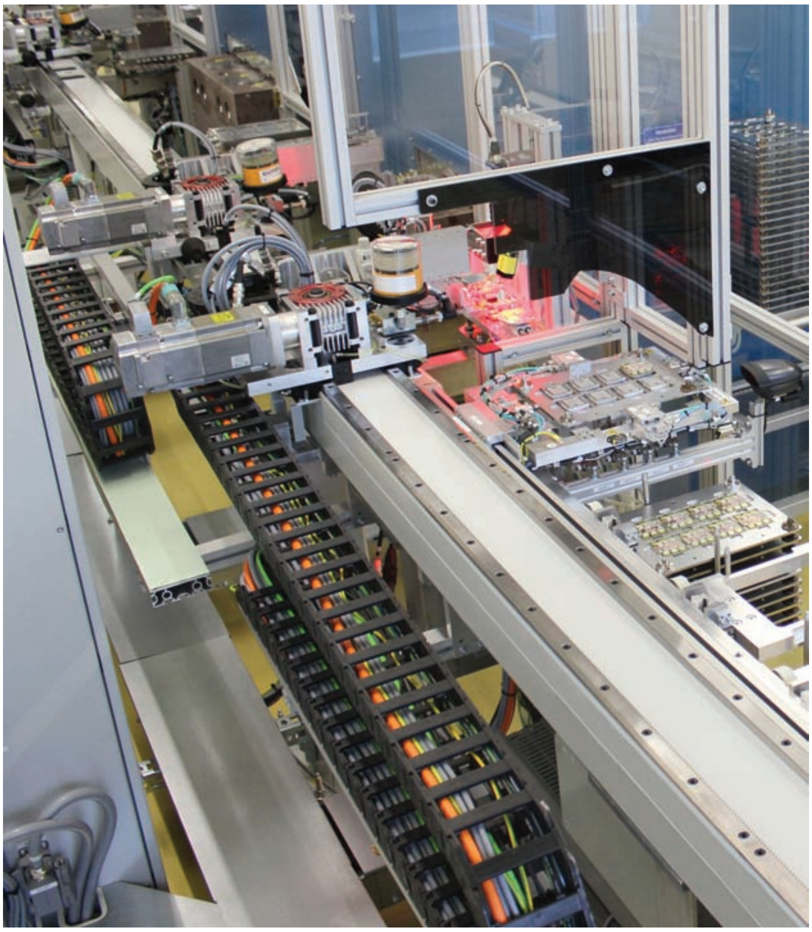

Figure 4: Substrate handling and conveyer for testing with 25°C static, 125°C dynamic and 125°C static

by limiting the current at device failure programmable test circuits to configure eg the stray inductance (down to 60 nH) in order to measure devices of different voltage classes; a programmable gate unit to cover a wide range of triggering capabilities; easily interchangeable barcode traceable snubber modules and the mechanical adaption of test fixtures within less than a minute to measure different device footprints; clamping devices of up to 240 mm in diameter with a clamping force of up to 240 kN; heating up to a precise temperature of the uniform clamped device of up to 200°C (production test systems) and a cooling down to a precise temperature of -40°C in an environmental chamber (engineering test systems).

Mechanical test system

In order to ensure outstanding reliability and failure-less operation of high-power semiconductors, not only electrical parameters but also mechanical specifications must be carefully monitored and controlled. One example is the baseplate flatness of IGBT modules. A test system as shown in Figure 2 enables the accurate, fast and reliable flatness measurement at predefined points of baseplates as incoming material or at finished products. The tests are performed at baseplates of up to 140 mm x 190 mm under nominal mounting conditions with an accuracy of better than 1 µm.

Visualization and automation

The control and visualization software together with a user friendly interface are crucial to both allowing for flexibility, enabling automation and offering easy programming. Setup verifications, test sequences, actions after measurement failures, setting of control limits, definition of sample plans and the programming of a configurable gate unit, signal generators and other peripheries are all to be programmed and visualized with the software. An example of a typical main user interface is shown in Figure 3. The test system and its software preferably also allow for direct or remote operation and must offer the capability of easy switching from the operator mode into the engineering or service mode.

To enhance production efficiency and improve quality the system shall take advantage of built-in barcode readers to control and verify the main test system configuration (eg snubber module fixture, active clamp module, etc) and read the measured device's part number, serial number, etc. It also shall interface with a manufacturing execution system (MES) to automatically download production orders with the corresponding test sequences as

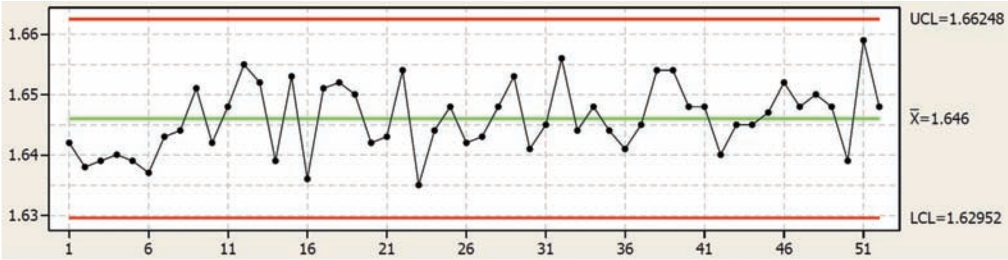

RIGHT Figure 5: Example of a SPC control chart

well as with a quality management system to upload the measured data for statistical process control (SPC, Figure 5). Automation and quality are both further improved by minimizing human interaction through integration of a sequence of different testers with conveyor belts as shown in Figure 4.

Quality

High quality products can only be delivered when tested with high quality testers. The careful and regular calibration of the test system is a prerequisite. A test system calibration includes the calibration of all electrical, mechanical, thermal and optical sensors. It also includes the verification of the clamping force of the press system, the pressure homogeneity, the mechanical centering, the alignment of the adapters, the temperatures, the voltage

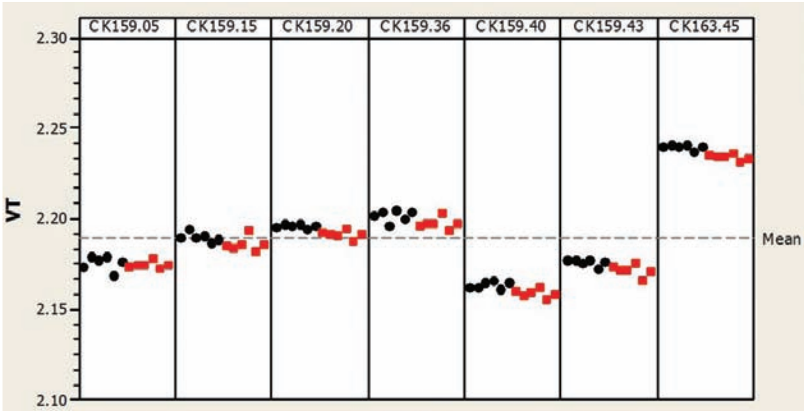

Figure 6: Example gage R&R for an on-state measurement on two static test systems

(AC/DC) and the current probes. Such a test system calibration is preferably done in collaboration with an independent national institute like the Swiss Federal Institute of Metrology. Repeatability and reproducibility of tests is ensured by frequent gage R&R control measurements (Figure 6).

IGBT Driver for Direct Press-Fit Mounting

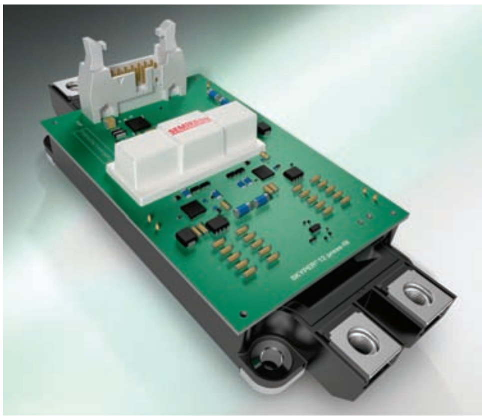

SEMIKRON's new SKYPER 12 press-fit half-bridge driver is pressed directly onto the IGBT module, which means that there are no costs for an adapter board, cable splices, and associated assembly and soldering processes. With 30 % fewer components than available solutions, the driver reduces the failure rate of the individual components and achieves an MTBF (mean time between failures as per SN 29500) rate of over 5 million hours at full load. This means that safe IGBT control is ensured even for the long working lives of industrial drives. A new generation of mixed-signal ASICs achieves a high level of integration. The ASIC chip set contains the power supply and protection and control functions, and the external components ensure optimum thermal spreading. Thanks to short pulse suppression and an interface ground concept, the usual good EMC stability of the SKYPER family is achieved. With square-wave signal transmission, the SKYPER 12 even switches without errors at a high dU/dt. The mixed-signal ASICs work in a stable manner over the entire temperature range with no transit time differences. The SKYPER 12 sits on 17 mm press-fit modules without an overhang and safely controls the modules up to a 15 A peak current and a DC link voltage of up to 1,200 V.

www.semikron.com

Digital Controlled 25A POL DC/DC Converter

Murata announced the first in a series of Point-of- Load non-isolated DC/DC converters based on the Digital Control Architecture from Powervation. The DOSA compatible OKLF 25A PoL has been designed to address the industry's growing requirement for low voltages (1.25 V and less), increased current and power densities, fast transient response times and the need for a tightly regulated DC output voltage. The first device in this new series is the OKLF-T/25-W12N-C. This PoL converter has been developed around a multi-processor System-on-Chip (SoC), digital power management IC from Powervation. The converter delivers a maximum of 25 A at 1.2 VDC out, when operating up to +70°C with a 200 LFM airflow. Also, this model has been designed to operate over a wide input voltage range of 6.5 to 14 VDC. The output voltage can be set in the range 0.69 V to 3.63 V using a single external resistor. The OKLF series has an ultra-fast dynamic load response feature that automatically compensates for various external conditions including capacitive loading, current steps, temperature, input voltage, and Vout setting.

www.murata.eu

3-Phase Current Transducer

The new RCTrms 3-ph current transducer from Power Electronic Measurements (PEM) delivers a convenient solution for measuring current in three phases. It features a thin, clip-around, flexible sensor coil and provides accurate true RMS measurement with 4-20mA or 0-5V output. The compact, DIN-rail or panel mountable RCTrms-3ph extends PEM's single-phase transducers, connecting to three Rogowski coils to capture measurements from three current phases simultaneously. With 18 current ratings options from 100 A to 50,000 A, and a choice of 300 mm, 500 mm, 700 mm or custom coil lengths, the RCTrms-3ph can be used in many applications and connected to a wide variety of SCADA systems, PLCs, data loggers, protection equipment or motor controllers. The clip-around coil design allows fast and easy positioning, and provides accurate results without needing to be centralized around the conductor. An isolated BNC-BNC cable-split option is available, to ease installation such as when threading through existing conduit.

www.pemuk.com

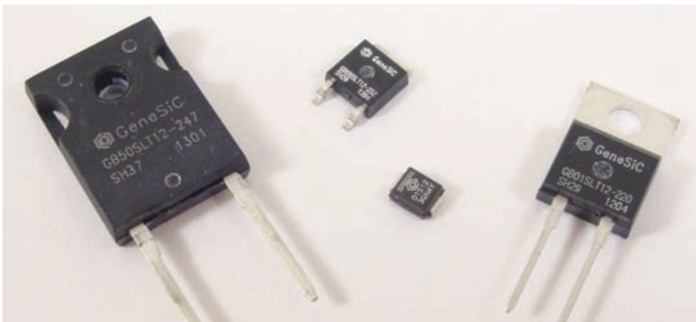

SiC Schottky Diodes in SMB Packages

GeneSiC Semiconductor offers a family of SMB (JEDEC DO-214AA) packaged SiC rectifiers in the 650 – 3300 V range. These products are targeted towards micro-solar inverters as well as voltage multiplier circuits used in a wide range of X-Ray, Laser and particle generator power supplies. The 650 V/1 A; 1200 V/2 A and 3300 V/0.3 A Schottky rectifiers feature zero reverse recovery current that does not change with temperature. The 3300 V-rated devices offer relatively high voltage in a single device allows a reduction in voltage multiplication stages required in typical high voltage generator circuits, through use of higher AC input voltages. The near-ideal switching characteristics allow the elimination/dramatic reduction of voltage balancing networks and snubber circuits. The SMB (DO-214AA) overmolded package features industry-standard form factor for surface mount assemblies.

www.genesicsemi.com/index.php/sic-products/schottky

AC/DC Connverters

www.irf.com
International Rectifier Co. (GB) Ltd
Tel: +44 (0)1737 227200

Arbitrary 4-Quadrant Power Sources

www.rohrer-muenchen.de
Rohrer GmbH
Tel.: +49 (0)89 8970120

Busbars

www.auxel.com
Auxel FTG
Tel: + 33 3 20 62 95 20

Capacitors

www.powersemiconductors.co.uk
Power Semiconductors Ltd
Tel: +44 (0)1727 811110

Certification

www.productapprovals.co.uk
Product Approvals Ltd
Tel: +44 (0)1588 620192

Connectors & Terminal Blocks

www.auxel.com
Auxel FTG
Tel: +44 (0)7714 699967

DC/DC Connverters

www.irf.com
International Rectifier Co. (GB) Ltd
Tel: +44 (0)1737 227200

DC/DC Connverters

www.power.ti.com
Texas Instruments
Tel: +44 (0)1604 663399

www.protocol-power.com
Protocol Power Products
Tel: +44 (0)1582 477737

Diodes

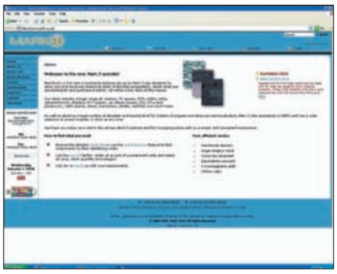

www.irf.com
International Rectifier Co. (GB) Ltd
Tel: +44 (0)1737 227200

www.mark5.com
Mark 5 Ltd
Tel: +44 (0)2392 618616

www.microsemi.com
Microsemi
Tel: 001 541 382 8028

www.neutronltd.co.uk
Neutron Ltd
Tel: +44 (0)1460 242200

www.voltagemultipliers.com
Voltage Multipliers, Inc.
Tel: 001 559 651 1402

www.proton-electrotex.com/
Proton-Electrotex JSC/
Tel: +7 4862 440642;

Direct Bonded Copper (DPC Substrates)

www.curamik.co.uk
curamik® electronics GmbH
Tel: +49 9645 9222 0

Discrete Semiconductors

www.digikey.com/europe
Digi-Key
Tel: +31 (0)53 484 9584

www.irf.com
International Rectifier Co. (GB) Ltd
Tel: +44 (0)1737 227200

www.microsemi.com
Microsemi
Tel: 001 541 382 8028

Drivers ICS

www.irf.com
International Rectifier Co. (GB) Ltd
Tel: +44 (0)1737 227200

www.power.ti.com
Texas Instruments
Tel: +44 (0)1604 663399

EMC/EMI

www.dextermag.com
Dexter Magnetic Technologies, Inc.
Tel: 001 847 956 1140

Ferrites & Accessories

www.dextermag.com
Dexter Magnetic Technologies, Inc.
Tel: 001 847 956 1140

Fuses

www.powersemiconductors.co.uk
Power Semiconductors Ltd
Tel: +44 (0)1727 811110

GTO/Triacs

www.mark5.com
Mark 5 Ltd
Tel: +44 (0)2392 618616

Hall Current Sensors

www.dgseals.com
dgseals.com
Tel: 001 972 931 8463

Harmonic Filters

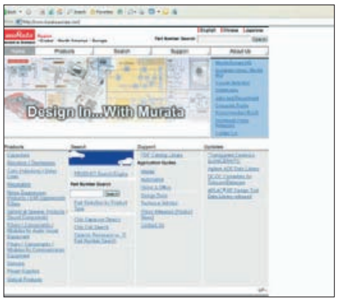

www.murata-europe.com
Murata Electronics (UK) Ltd
Tel: +44 (0)1252 811666

IGBTs

www.irf.com
International Rectifier Co. (GB) Ltd
Tel: +44 (0)1737 227200

www.microsemi.com
Microsemi
Tel: 001 541 382 8028

www.neutronltd.co.uk
Neutron Ltd
Tel: +44 (0)1460 242200

www.irf.com
International Rectifier Co. (GB) Ltd
Tel: +44 (0)1737 227200

www.power.ti.com
Texas Instruments
Tel: +44 (0)1604 663399

Line Simulation

www.hero-power.com
Rohrer GmbH
Tel.: +49 (0)89 8970120

Magnetic Materials/Products

www.dextermag.com
Dexter Magnetic Technologies, Inc.
Tel: 001 847 956 1140

www.rubadue.com
Rubadue Wire Co., Inc.
Tel. 001 970-351-6100

Mosfets

www.irf.com
International Rectifier Co. (GB) Ltd
Tel: +44 (0)1737 227200

www.mark5.com
Mark 5 Ltd
Tel: +44 (0)2392 618616

www.microsemi.com
Microsemi
Tel: 001 541 382 8028

www.neutronltd.co.uk
Neutron Ltd
Tel: +44 (0)1460 242200

Optoelectronic Devices

www.digikey.com/europe
Digi-Key Tel: +31 (0)53 484 9584

www.power.ti.com
Texas Instruments
Tel: +44 (0)1604 663399

Packaging & Packaging Materials

www.curamik.co.uk
curamik® electronics GmbH
Tel: +49 9645 9222 0

Power Amplifiers

www.rohrer-muenchen.de
Rohrer GmbH
Tel.: +49 (0)89 8970120

Power ICs

www.digikey.com/europe
Digi-Key Tel: +31 (0)53 484 9584

www.irf.com
International Rectifier Co. (GB) Ltd
Tel: +44 (0)1737 227200

www.power.ti.com
Texas Instruments
Tel: +44 (0)1604 663399

Power Modules

www.auxel.com
Auxel FTG
Tel: +44 (0)7714 699967

www.irf.com
International Rectifier Co. (GB) Ltd
Tel: +44 (0)1737 227200

www.microsemi.com
Microsemi
Tel: 001 541 382 8028

www.power.ti.com
Texas Instruments
Tel: +44 (0)1604 663399

www.proton-electrotex.com/
Proton-Electrotex JSC/
Tel: +7 4862 440642;

Power Protection Products

www.power.ti.com
Texas Instruments
Tel: +44 (0)1604 663399

Power Semiconductors

www.proton-electrotex.com/
Proton-Electrotex JSC/
Tel: +7 4862 440642;

Power Substrates

www.universal-science.com
Universal Science Ltd
Tel: +44 (0)1908 222211

Resistors & Potentiometers

www.isabellenhuette.de
Isabellenhütte Heusler GmbH KG
Tel: +49/(27 71) 9 34 2 82

RF & Microwave Test Equipment.

www.ar-europe.ie
AR Europe
Tel: 353-61-504300

Simulation Software

www.power.ti.com
Texas Instruments
Tel: +44 (0)1604 663399

www.universal-science.com
Universal Science Ltd
Tel: +44 (0)1908 222211

Smartpower Devices

www.irf.com
International Rectifier Co. (GB) Ltd
Tel: +44 (0)1737 227200

Switches & Relays

www.irf.com
International Rectifier Co. (GB) Ltd
Tel: +44 (0)1737 227200

Switched Mode Power Supplies

www.biaspower.com
Bias Power, LLC
Tel: 001 847 215 2427

Switched Mode Power Supplies

www.power.ti.com
Texas Instruments
Tel: +44 (0)1604 663399

Thermal Management & Heatsinks

www.abl-heatsinks.co.uk
ABL Components Ltd
Tel: +44 (0) 121 789 8686

www.curamik.co.uk
curamik® electronics GmbH
Tel: +49 9645 9222 0

www.dau-at.com
Dau GmbH & Co KG
Tel: +43 3143 23510

www.power.ti.com
Texas Instruments
Tel: +44 (0)1604 663399

www.universal-science.com
Universal Science Ltd
Tel: +44 (0)1908 222211

Thyristors

www.irf.com
International Rectifier Co. (GB) Ltd
Tel: +44 (0)1737 227200

www.mark5.com
Mark 5 Ltd
Tel: +44 (0)2392 618616

www.proton-electrotex.com/
Proton-Electrotex JSC/
Tel: +7 4862 440642;

Voltage References

www.irf.com
International Rectifier Co.
(GB) Ltd
Tel: +44 (0)1737 227200

ADVERTISERS INDEX

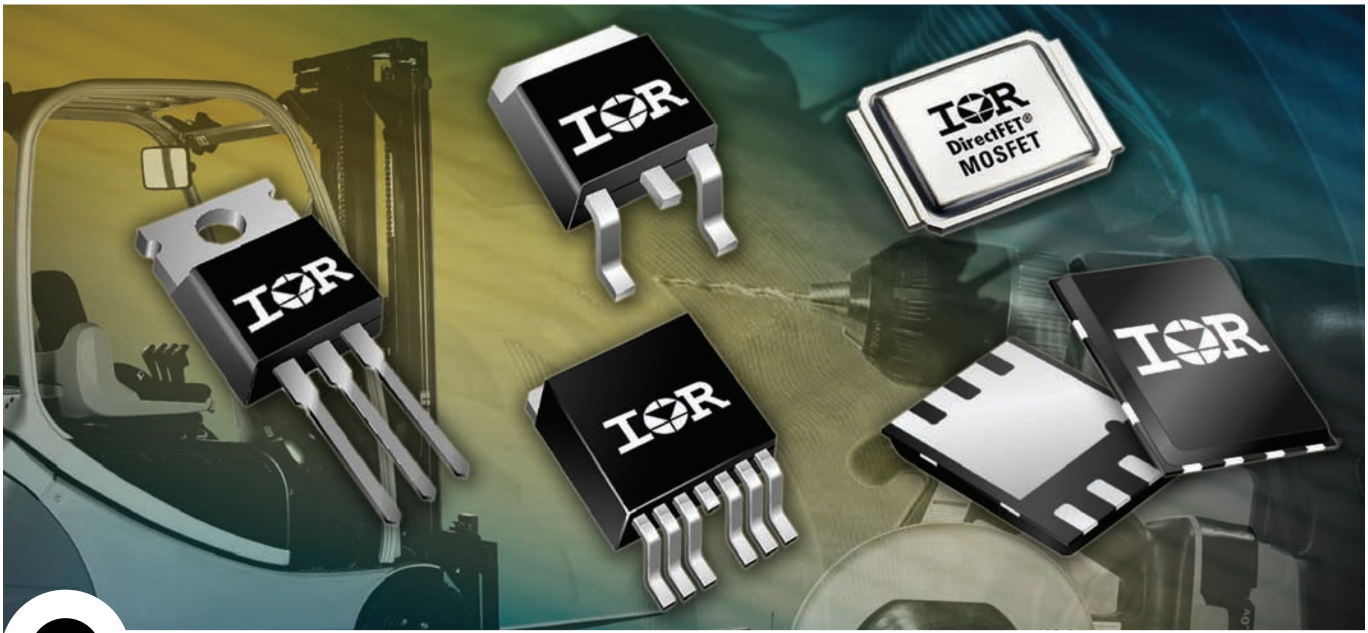

StrongIRFET™ Rugged, Reliable MOSFETs

Specifications

Part Number	B_{VDSS}	ID@ 25°C	$R_{DS(on)}$ max@ Vgs = 10V	Qg@ Vgs = 10V	Package
IRFH7004TRPbF	40 V	100 A	1.4 mΩ	134 nC	PQFN 5x6
IRFH7440TRPbF	40 V	85 A	2.4 mΩ	92 nC	PQFN 5x6
IRFH7446TRPbF	40 V	85 A	3.3 mΩ	65 nC	PQFN 5x6
IRF7946TRPbF	40 V	90 A	1.4 mΩ	141 nC	DirectFET Medium Can
IRFS7437TRLPbF	40 V	195 A	1.8 mΩ	150 nC	D^2-Pak
IRFS7440TRLPbF	40 V	120 A	2.8 mΩ	90 nC	D^2-Pak
IRFS7437TRL7PP	40 V	195 A	1.5 mΩ	150 nC	D^2-Pak 7pin
IRFR7440TRPbF	40 V	90 A	2.5 mΩ	89 nC	D-Pak
IRFB7430PbF	40 V	195 A	1.3 mΩ	300 nC	TO-220AB
IRFB7434PbF	40 V	195 A	1.6 mΩ	216 nC	TO-220AB
IRFB7437PbF	40 V	195 A	2 mΩ	150 nC	TO-220AB
IRFB7440PbF	40 V	120 A	2.5 mΩ	90 nC	TO-220AB
IRFB7446PbF	40 V	118 A	3.3 mΩ	62 nC	TO-220AB
IRFP7430PbF	40 V	195 A	1.3 mΩ	300 nC	TO-247

Features:

- Ultra low $R_{DS(on)}$
- High current capability
- Industrial qualified
- Broad portfolio offering

Applications:

- Battery Packs
- Inverters
- UPS
- Solar Inverter
- DC Motors
- ORing or Hotswap